CHAPTER III
RESULTS

3.1 Cell behavior and morphology

3.1.1 Fibroblasts culture established from *Cspg2*$^{\Delta 3/\Delta 3}$ embryo

To produce fibroblasts culture, a transgenic *Cspg2*$^{\Delta 3/\Delta 3}$ mice were constructed by Professor Dr. Koji Kimata's Laboratory. First, a mouse 129SVj strain genomic library was screened for mouse versican cDNA and isolated (Shinomura *et al.,* 1993), then gene targeting was performed by the PGK promoter-*neo*$_r$-polyA cassette from pPNT was inserted into an *NcoI* site in exon3 of targeting vector, which encodes the A subdomain of the G1 domain. This new constructed gene contained the translational start site in exon 2, and skipping exon 3 results in the "in frame" synthesis of versican without the A subdomain as shown in figure 3.1. The targeting vector was linearized by *NotI* digestion, afterwards it was transfected into the embryonic cell (E14TG2) via electroporation method, the transfected cells were selected and sent to private scientific organization to produce the chimera mouse, the chimeras were generated by blastocyst injection of heterozygous embryonic stem cells. Male chimeras were capable of germ line transmission of the mutant allele. Heterozygous progeny was maintained as a hybrid of C57Bl/6; 129Svj strain, then backcrossed to C57Bl/6 strain, and crossed to Balb/c strain. The heterozygous progeny as showed in figure 3.2, was sent back to laboratory,then homozygous progeny was generated by crossing between heterozygous *Cspg2*$^{\Delta 3/\Delta 3}$ male

ลิขสิทธิ์มหาวิทยาลัยเชียงใหม่
Copyright© by Chiang Mai University
All rights reserved

and female mouse. Embryos at 11.5 days as demonstrated in figure 3.2 were isolated from pregnant mouse, then chopped and digested with trypsin/EDTA to dissociate fibroblast cells from tissue. At this stage, the whole embryo composes of fibroblast cells only. The isolated fibroblasts were cultured in DMEM containing 10% FBS, 1% penicillin/streptomycin in CO_2 incubator under 95% air, 5% CO_2, at 37 ˚C , and contamination was observed, the non-contaminated fibroblasts cultures were collected and maintained for further experiments.

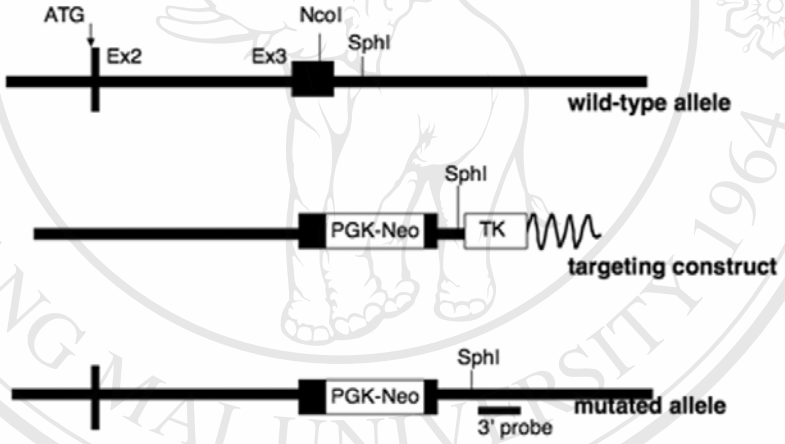

Figure 3.1 The genomic organization of *Cspg2*$^{\Delta 3/\Delta 3}$, the targeting vector, and the mutated allele by homologous recombinant. The vector was constructed so that PGK-*neo*$_r$ was inserted into exon 3.

ลิขสิทธิ์มหาวิทยาลัยเชียงใหม่
Copyright© by Chiang Mai University
All rights reserved

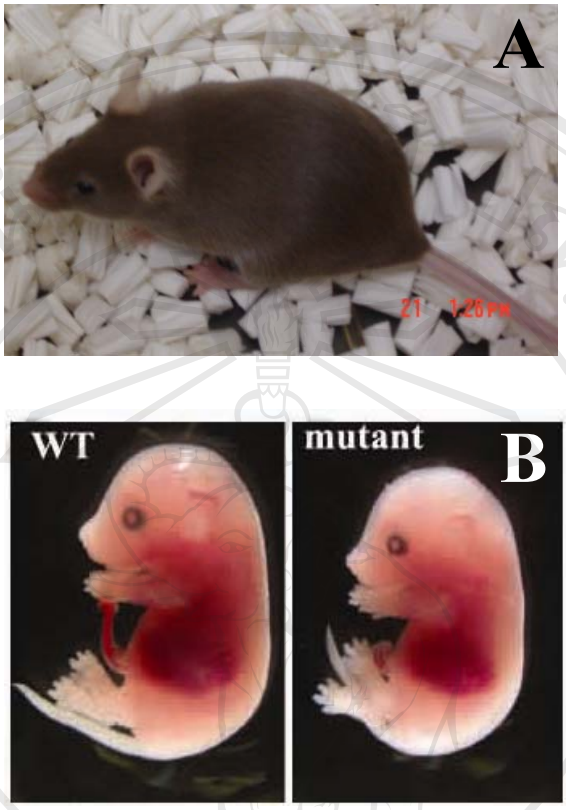

Figure 3.2 Phenotype of *Cspg2* gene modified mouse and embryo. A: The heterozygous A subdomain less versican ($Cspg2^{WT/\Delta 3}$) producing mouse. B: The homozygous A subdomain less versican (mutant, $Cspg2^{\Delta 3/\Delta 3}$) producing mouse embryo at day 11.5 compares with WT mouse embryo at the same day.

ลิขสิทธิ์มหาวิทยาลัยเชียงใหม่
Copyright© by Chiang Mai University
All rights reserved

The genotype of embryo was characterized by using genomic PCR technique, cDNA was extracted from embryo tail, and PCR was performed. There are two primers sets used for genotype characterization including WT allele, heterozygous mutant allele, and homozygous mutant allele. The genotyping results are showed in figure 3.3, the PCR products from WT allele showed a positive band for WT primers, vice versa to homozygous mutant allele, a band was appeared for mutant primers. In case of heterozygous mutant allele, bands were appeared for both WT and mutant primers. From the results, it was suggested that the WT allele was embryos No. 1, 4, 8, 15, 21, but embryos No 6, 12, 19, 22 were homozygous allele, while the rest embryos were heterozygous allele. These results will be used for selecting fibroblasts cultures to perform further experiments.

ลิขสิทธิ์มหาวิทยาลัยเชียงใหม่
Copyright© by Chiang Mai University
All rights reserved

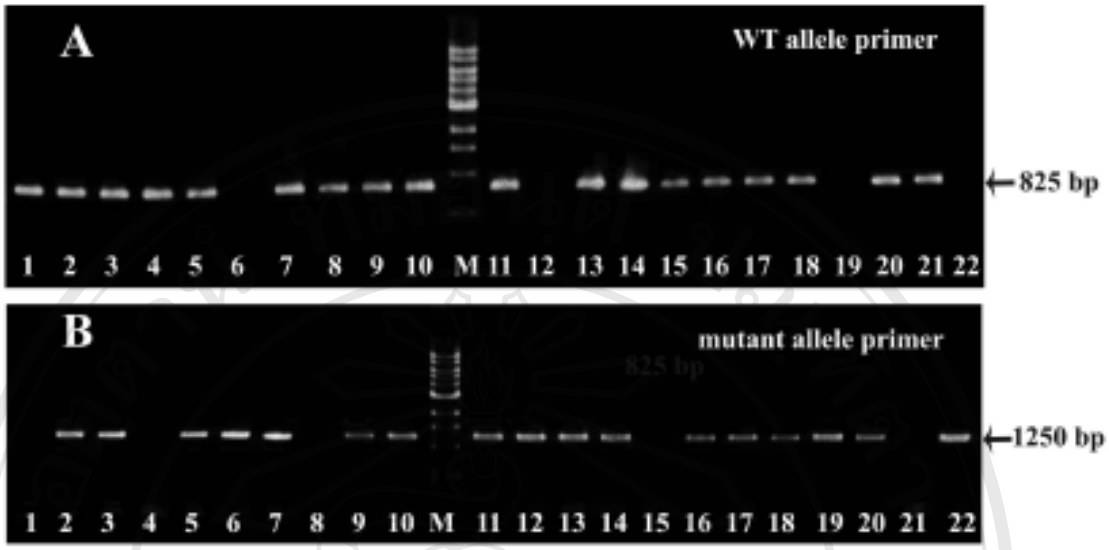

Figure 3.3 Agarose gel electrophoresis of PCR products from mice embryo tails, each lane in figures A and B represents PCR product from embryo. A, gel electrophoresis of PCR products from embryo's cDNA samples were added to PCR mixture containing WT allele primers. B, gel electrophoresis of PCR products from embryo's cDNA samples were added to PCR mixture containing mutant allele primers. Lane 1 – 10: Embryo No. 1 – 10, Lane M: 1 kb DNA ladder, Lane 11 – 22, Embryo No. 11 – 22, respectively.

ลิขสิทธิ์มหาวิทยาลัยเชียงใหม่
Copyright© by Chiang Mai University
All rights reserved

From observation, heterozygous *Cspg2*$^{wt/\Delta 3}$ mice were viable, fertile, and without obvious abnormalities from WT mice, but no *Cspg2*$^{\Delta 3/\Delta 3}$ homozygote was borned. The homozygote embryos expressed abnormality in cardiovascular system, and relative smaller than WT. Therefore, only homozygote allele was selected to study the abnormalities. From genomic PCR results, fibroblasts containing WT and homozygous allele were cultured. At the early passages of both fibroblasts alleles (passages 1-10), WT fibroblasts morphology differed from the *Cspg2*$^{\Delta 3/\Delta 3}$ fibroblasts. The *Cspg2*$^{\Delta 3/\Delta 3}$ fibroblasts appeared larger, more flat and spread than WT fibroblasts in both low and high cell density as illustrated in figure 3.4. Interestingly, the *Cspg2*$^{\Delta 3/\Delta 3}$ fibroblasts reached to the confluence later compared to WT fibroblasts. It was assumed that proliferation rate of the *Cspg2*$^{\Delta 3/\Delta 3}$ fibroblasts might be slower than WT fibroblasts, and cellular activities of these fibroblasts were changed, thus proliferation rate and cellular activities in the *Cspg2*$^{\Delta 3/\Delta 3}$ fibroblasts was subjected to be investigated.

ลิขสิทธิ์มหาวิทยาลัยเชียงใหม่
Copyright© by Chiang Mai University
All rights reserved

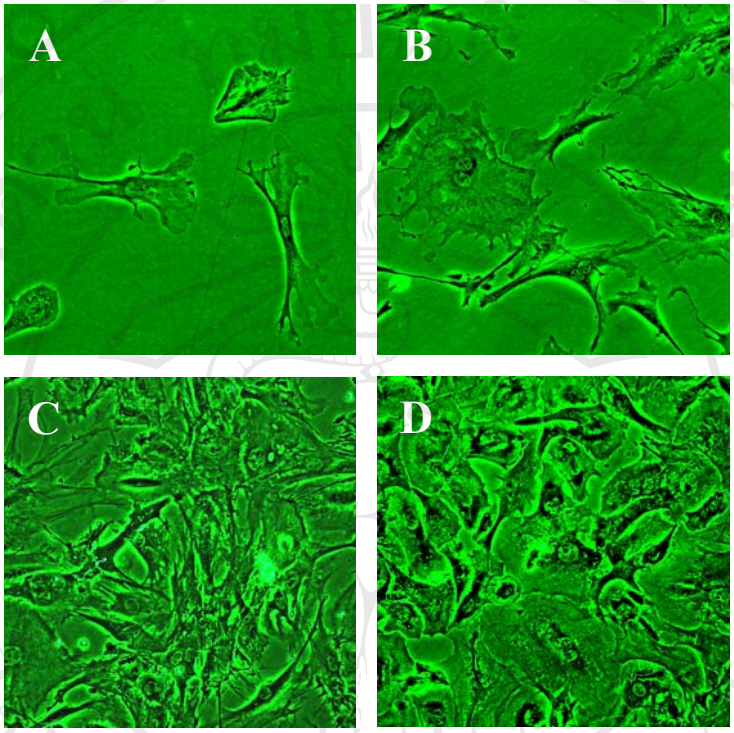

Figure 3.4 Morphology of the WT and *Cspg2*$^{\Delta 3/\Delta 3}$ fibroblasts at passages 5 (10X magnification), WT fibroblasts at low (A) and high (C) density. *Cspg2*$^{\Delta 3/\Delta 3}$ fibroblasts at low (B) and high (D) density.

ลิขสิทธิ์มหาวิทยาลัยเชียงใหม่
Copyright© by Chiang Mai University
All rights reserved

3.1.2 *Cspg2*$^{\Delta 3/\Delta 3}$ fibroblasts expressed low proliferation rate and premature senescence characteristic at early passages.

As the *Cspg2*$^{\Delta 3/\Delta 3}$ fibroblasts reaching to confluence slower than WT, it took around two weeks to reach confluence for *Cspg2*$^{\Delta 3/\Delta 3}$ fibroblasts at early passages, whereas 4-5 days for WT. Therefore to demonstrate this phenomenon, proliferation rate of MEFs, both WT and *Cspg2*$^{\Delta 3/\Delta 3}$, was measured. The BrdU ELISA assay was used to determine proliferation rate by detecting BrdU incorporation rate. Cells were cultured in DMEM containing BrdU, then BrdU will be incorporated and used as a substrate to produce DNA, high proliferating cells required BrdU more than low proliferating cell. Comparing BrdU incorporating rate of WT compared to *Cspg2*$^{\Delta 3/\Delta 3}$ fibroblasts at passages 5, the *Cspg2*$^{\Delta 3/\Delta 3}$ fibroblasts showed ~50% BrdU incorporation that of WT fibroblasts at a comparable number of passages as showed in Figure 3.5, it was suggested that proliferation rate of the *Cspg2*$^{\Delta 3/\Delta 3}$ fibroblasts was slower than WT fibroblasts.

To confirm BrdU ELISA assay result, cell counting assay was performed. Fibroblasts (2×10^4 cells) were plated onto six-well plates and cultured in DMEM containing 10% FBS, 1% penicillin/streptomycin. The cell number was counted at day 1-6, using a hemocytometer. The result as demonstrated in figure 3.6 corresponded to previous result, however cell number of WT fibroblasts on day 1-4 was not different to *Cspg2*$^{\Delta 3/\Delta 3}$ fibroblasts but at day 5 and 6 cell number of WT fibroblasts was higher than *Cspg2*$^{\Delta 3/\Delta 3}$ fibroblasts.

ลิขสิทธิ์มหาวิทยาลัยเชียงใหม่
Copyright© by Chiang Mai University
All rights reserved

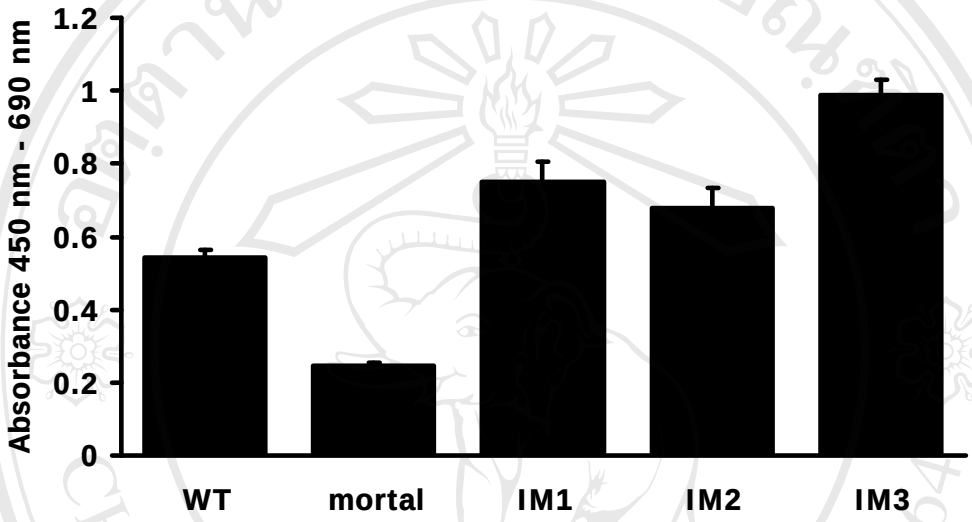

Figure 3.5 Proliferation rates of MEFs at different phenotype were measured by BrdU incorporation ELISA assay. WT = wild type at passages 5, mortal = *Cspg2*$^{\Delta 3/\Delta 3}$ at early passages 5, IM1 = transformed *Cspg2*$^{\Delta 3/\Delta 3}$ No. 1, IM2 = transformed *Cspg2*$^{\Delta 3/\Delta 3}$ No. 2, IM3 = transformed *Cspg2*$^{\Delta 3/\Delta 3}$ No. 3. All values represent the mean $\pm$ SD in triplicate.

ลิขสิทธิ์มหาวิทยาลัยเชียงใหม่
Copyright© by Chiang Mai University
All rights reserved

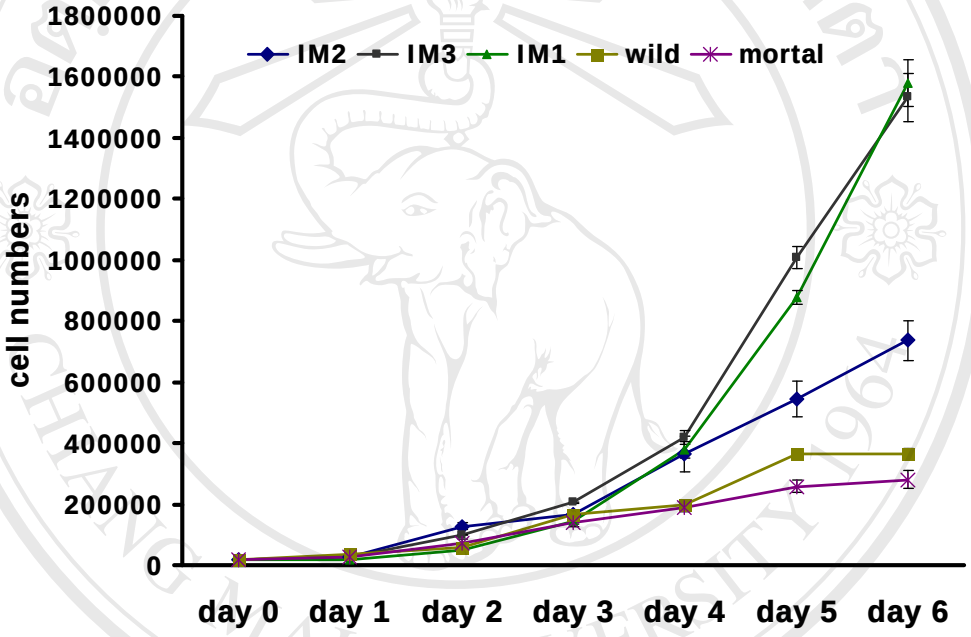

Figure 3.6 Proliferation rates of MEFs at different phenotype were measured by cell counting assay. WT = wild type at passages 5, mortal = *Cspg2*$^{\Delta 3/\Delta 3}$ at passages 5, IM1 = transformed *Cspg2*$^{\Delta 3/\Delta 3}$ No. 1, IM2 = transformed *Cspg2*$^{\Delta 3/\Delta 3}$ No. 2, IM3 = transformed *Cspg2*$^{\Delta 3/\Delta 3}$ No. 3. All values represent the mean $\pm$ SD in triplicate.

ลิขสิทธิ์มหาวิทยาลัยเชียงใหม่
Copyright© by Chiang Mai University
All rights reserved

As *Cspg2*$^{\Delta 3/\Delta 3}$ fibroblasts at the early passages exhibited low proliferation rate, larger, more flat and spread simultaneously. This incident resembled to a cellular senescence phenomenon, the state in which normal cells irreversibly stop dividing itself. Remarkably, the *Cspg2*$^{\Delta 3/\Delta 3}$ fibroblasts entered to senescent stage at early passages or premature senescence whereas the normal fibroblasts or other primary cells entered to senescent stage when they reached overpassages 20. However, the premature senescent cells can be found in cells defective in tumor suppressor genes. To investigate whether *Cspg2*$^{\Delta 3/\Delta 3}$ fibroblasts exhibit premature senescent character, β-galactosidase activity staining assay was performed. In this experiment, β-galactosidase activity was performed at pH 6.0, at this pH only senescence associated β-galactosidase was able to express its activity. Cells expressing a β-galactosidase will be detected by X-gal, which form a local blue precipitate upon cleavage. Figure 3.7 showed that the *Cspg2*$^{\Delta 3/\Delta 3}$ fibroblasts at passages five presented obviously blue precipitate in cytoplasm, compared to the WT fibroblasts. Hence, *Cspg2*$^{\Delta 3/\Delta 3}$ fibroblasts expressed high β-galactosidase activity, which is the cellular senescence marker. Together with morphology observation, BrdU ELISA assay for DNA synthesis, and β-galactosidase activity staining, suggested that *Cspg2*$^{\Delta 3/\Delta 3}$ fibroblasts entered to senescent stage at early passages. Entering to senescent stage of *Cspg2*$^{\Delta 3/\Delta 3}$ fibroblasts at early stage caused changing in cell morphology and reduced proliferation rate (entered to growth arrest stage).

ลิขสิทธิ์มหาวิทยาลัยเชียงใหม่
Copyright© by Chiang Mai University
All rights reserved

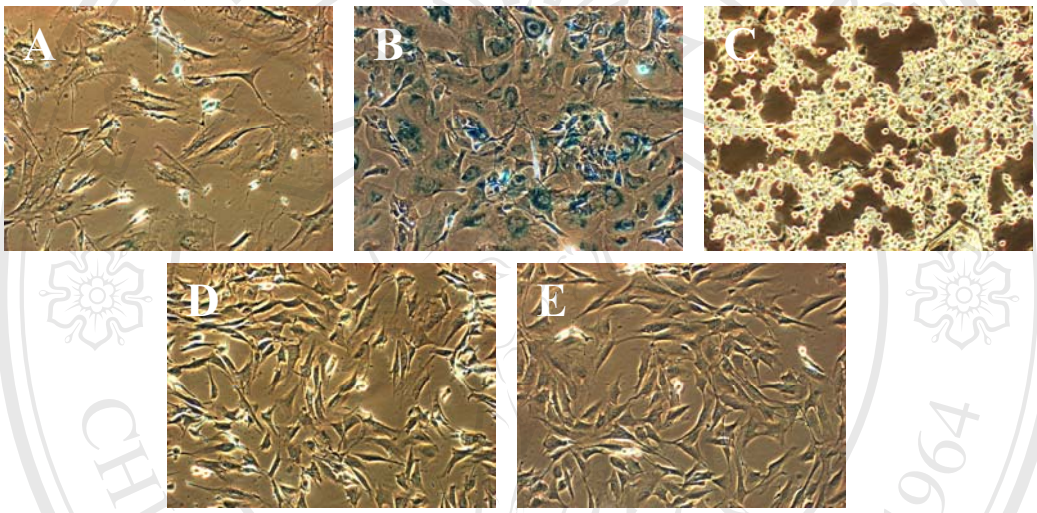

Figure 3.7 Staining of β-galactosidase activity in fibroblasts culture. Fibroblasts were cultured in 36 mm dish until reached to confluence, then β-galactosidase activity was stained, the stained fibroblasts were photographed at 10X magnification through microscope. A = WT at passages 5, B = *Cspg2*$^{\Delta 3/\Delta 3}$ at passages 5, C = transformed *Cspg2*$^{\Delta 3/\Delta 3}$ No.1, D = transformed *Cspg2*$^{\Delta 3/\Delta 3}$ No.2, E = transformed *Cspg2*$^{\Delta 3/\Delta 3}$ No.3.

ลิขสิทธิ์มหาวิทยาลัยเชียงใหม่
Copyright© by Chiang Mai University
All rights reserved

3.1.3 *Cspg2*$^{\Delta 3/\Delta 3}$ fibroblasts escaped from senescence, and expressed high proliferation rate after growing more than ten passages.

The premature senescent *Cspg2*$^{\Delta 3/\Delta 3}$ fibroblasts were cultured in DMEM supplemented with 10% FBS, 1% penicillin/streptomycin. More interestingly, when *Cspg2*$^{\Delta 3/\Delta 3}$ fibroblasts grew over than ten passages, cell morphology and proliferation rate was changed. This event was differ from normal primary cells such as the WT fibroblasts, when they grew for several passages, proliferation rate decreased and doom to die which is a characteristic of primary fibroblasts which enter to senescent stage and die after growing for several passages.

To observe changing in cell morphology and growth rate of *Cspg2*$^{\Delta 3/\Delta 3}$ fibroblasts, the *Cspg2*$^{\Delta 3/\Delta 3}$ and WT fibroblasts were cultured, proliferation rate and cell morphology in each passages were observed using BrdU ELISA assay, and microscope respectively. As shown in figure 3.8, passage number and proliferation rate were plotted. It was found that at early passages proliferation rate of WT fibroblasts was higher than of *Cspg2*$^{\Delta 3/\Delta 3}$ fibroblasts. However when passage went by, a proliferation rate was decreased until passaged through over than 20, they stopped growing and died. Considering to cell morphology, after growing for several passages, WT fibroblast cell enlarged and flatten, that was sign of senescence cell as illustrated in figure 3.9. At the same time, the *Cspg2*$^{\Delta 3/\Delta 3}$ fibroblasts expressed low proliferation rate, large and flatten at early passages that is a senescent characteristic. Interestingly, when passages went by, most cells rather synchronically began to proliferate. These cells became smaller,

ลิขสิทธิ์มหาวิทยาลัยเชียงใหม่
Copyright© by Chiang Mai University
All rights reserved

less spread, and more elongated in the growing phase as depicted in figure 3.10. For proliferation rate of *Cspg2*$^{\Delta 3/\Delta 3}$ fibroblasts, it was dramatically higher and tended to stable after growing for more than 50 passages. These transformed *Cspg2*$^{\Delta 3/\Delta 3}$ fibroblasts kept growing with very highly proliferation rate and seemed growing without limitation, They proliferated over the confluence and piled up to several layers, indicating loss of the contact inhibition. Several lots of the *Cspg2*$^{\Delta 3/\Delta 3}$ fibroblasts from different mothering mice were grown to confirm these results. The results showed that every lot of *Cspg2*$^{\Delta 3/\Delta 3}$ fibroblasts cultures expressed in the same manner, they tended to change their morphology and proliferation rate after growing over than ten passages. It was suggested that the *Cspg2*$^{\Delta 3/\Delta 3}$ fibroblasts escaped from senescence and immortalized.

To verify whether transformed *Cspg2*$^{\Delta 3/\Delta 3}$ fibroblasts escape from senescence stage, β-galactosidase activity staining assay was performed. As shown in figure 3.7, the transformed *Cspg2*$^{\Delta 3/\Delta 3}$ fibroblasts at passages over than 30 which obtained from three different lots can not be stained by blue precipitate from X-gal, interestingly, the transformed *Cspg2*$^{\Delta 3/\Delta 3}$ fibroblasts number1 (IM1) presented a brighter and smaller cell than transformed *Cspg2*$^{\Delta 3/\Delta 3}$ fibroblasts number 2 (IM2) and number3 (IM3) when observed under light microscope as depicted in figure 3.9. According to proliferation rate, was determined by BrdU ELISA assay, and cell counting assay, it was found that proliferation rates of all three transformed *Cspg2*$^{\Delta 3/\Delta 3}$ fibroblasts were higher than non-transformed *Cspg2*$^{\Delta 3/\Delta 3}$ fibroblasts (early passages *Cspg2*$^{\Delta 3/\Delta 3}$ fibroblasts) or WT fibroblasts, results were shown in figure 3.5 and 3.6. These results revealed that those *Cspg2*$^{\Delta 3/\Delta 3}$ fibroblasts escaped from senescent stage.

ลิขสิทธิ์มหาวิทยาลัยเชียงใหม่
Copyright© by Chiang Mai University
All rights reserved

To confirm that the *Cspg2*$^{\Delta 3/\Delta 3}$ fibroblasts remained a defect in exon 3 in versican gene though had transformed, genomic PCR was performed again in WT and three lots of transformed *Cspg2*$^{\Delta 3/\Delta 3}$ fibroblasts at passages over than 30, genomic DNA from WT and homozygous *Cspg2*$^{\Delta 3/\Delta 3}$ mouse embryos were used to be a control (proper versican gene) and exon 3 defected versican gene respectively. The result presented in figure 3.10 showed that all three lots of transformed *Cspg2*$^{\Delta 3/\Delta 3}$ fibroblasts still maintained versican gene with disrupted exon 3.

ลิขสิทธิ์มหาวิทยาลัยเชียงใหม่
Copyright© by Chiang Mai University
All rights reserved

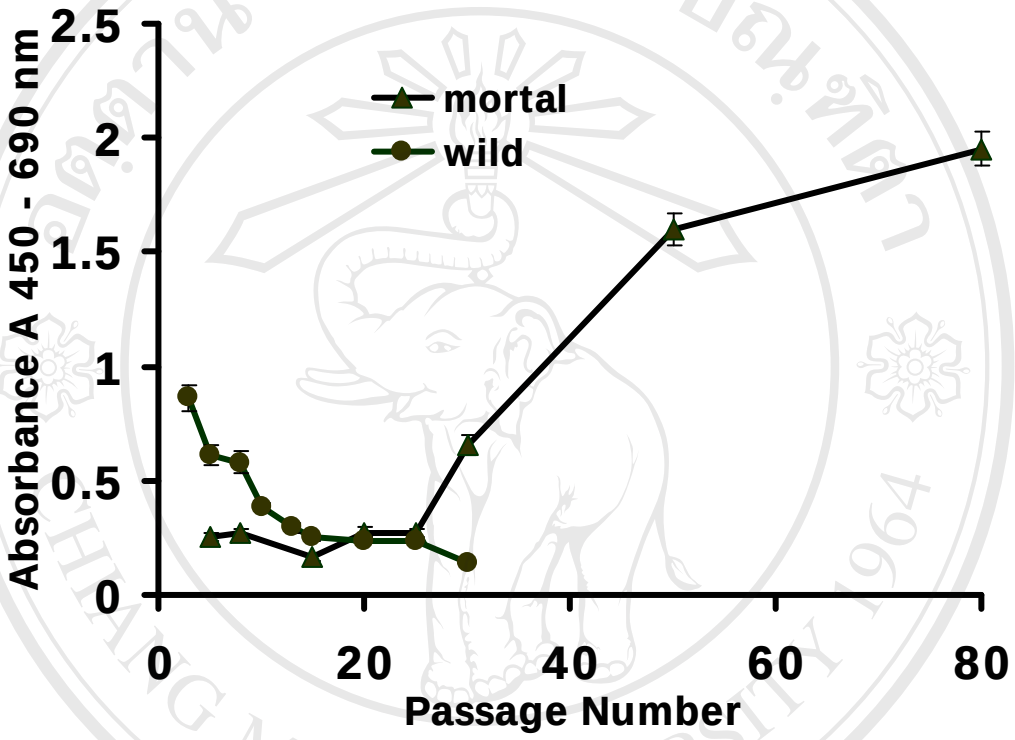

Figure 3.8 Proliferation rates of MEFs in each passage. WT and *Cspg2*$^{\Delta 3/\Delta 3}$ fibroblasts were cultured, the proliferation rate was detected along the passages. All values represent the mean ± SD in triplicate.

ลิขสิทธิ์มหาวิทยาลัยเชียงใหม่
Copyright© by Chiang Mai University
All rights reserved

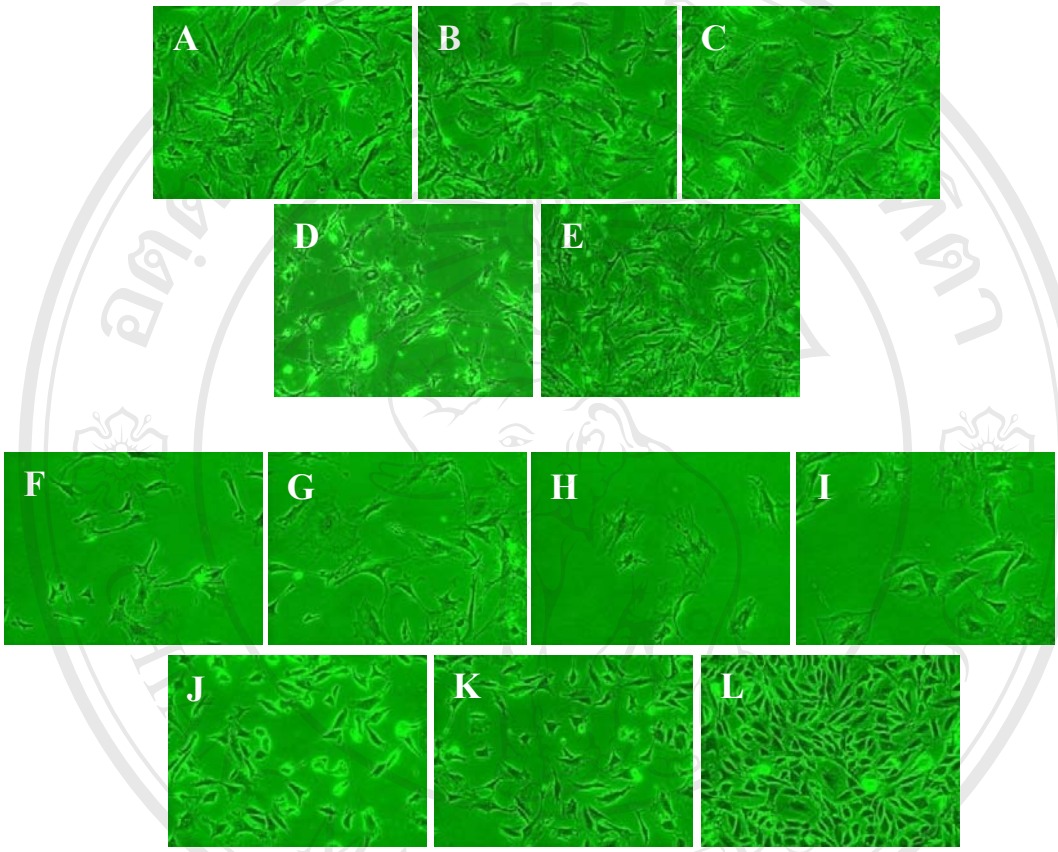

Figure 3.9 Morphology of MEFs in each passage. WT (A-E) and *Cspg2*$^{\Delta 3/\Delta 3}$ (F-L) fibroblasts were cultured, the morphology was observed and photographed along the passages. A = passages 3, B = passages 5, C = passages 10, D = passages 15, E = passages 22, F = passages 5, G = passages 8, H = passages 15, I = passages 20, J = passages 25, K = passages 30, L = passages 50.

ลิขสิทธิ์มหาวิทยาลัยเชียงใหม่
Copyright© by Chiang Mai University
All rights reserved

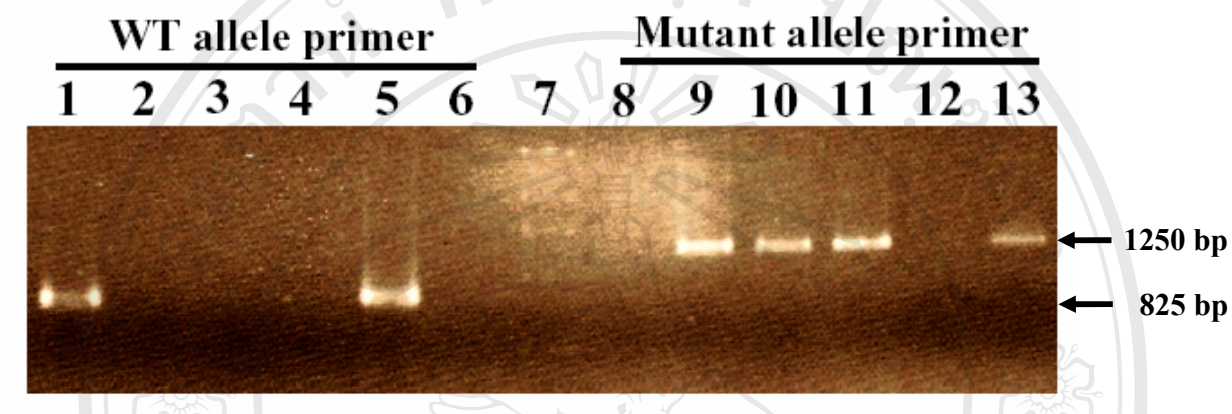

Figure 3.10 Agarose Gel electrophoresis of PCR products from fibroblasts culture, each lane represents PCR product from fibroblasts as following, 1 = WT, 2 = transformed *Cspg2*$^{\Delta 3/\Delta 3}$ (IM1), 3 = transformed *Cspg2*$^{\Delta 3/\Delta 3}$ (IM2), 4 = transformed *Cspg2*$^{\Delta 3/\Delta 3}$ (IM3), 5 = WT allele gene template (850 bp), 6 = mutant allele gene template (1250 bp), 7 = 1 kb DNA marker, 8 = WT, 9 = transformed *Cspg2*$^{\Delta 3/\Delta 3}$ (IM1), 10 = transformed *Cspg2*$^{\Delta 3/\Delta 3}$ (IM2), 11 = transformed *Cspg2*$^{\Delta 3/\Delta 3}$ (IM3), 12 = WT allele gene template (850 bp), 13 = mutant allele gene template (1250 bp). PCR in lane one to six was performed with WT allele primer, whereas lane 8-13 were performed with mutant allele primer.

ลิขสิทธิ์มหาวิทยาลัยเชียงใหม่
Copyright© by Chiang Mai University
All rights reserved

3.1.4 The transformed *Cspg2*$^{\Delta 3/\Delta 3}$ fibroblasts were malignant cells.

According to the results in 3.1.3, the transformed *Cspg2*$^{\Delta 3/\Delta 3}$ fibroblasts not only escaped from senescent stage but grew substantially rapid and piled up. Cell behavior was similar to malignant cells. To investigate whether transformed *Cspg2*$^{\Delta 3/\Delta 3}$ fibroblasts are malignant cells, experiments to collaborate this incidence were performed. The experiments consist of soft agarose gel cultivation and implantation of the transformed *Cspg2*$^{\Delta 3/\Delta 3}$ fibroblasts to nude mice.

For the first experiment, WT, early passages *Cspg2*$^{\Delta 3/\Delta 3}$ and transformed *Cspg2*$^{\Delta 3/\Delta 3}$ fibroblasts were cultured on soft agarose culture to determine anchorage-independent growth characteristic. Typically, primary cells have anchorage-dependent character, thus they can not grow and survive under condition without anchorage materials, contrasting to the transformed or malignant cells could grow even under condition without anchorage materials. The results shown in figure 3.11 showed that, as expected WT cells died after had been cultured for one week whereas early passages *Cspg2*$^{\Delta 3/\Delta 3}$ fibroblasts aggregated to each other, then doomed to die within one week, likewise in WT fibroblasts. Meanwhile, IM1 and IM3, but not IM2 transformed *Cspg2*$^{\Delta 3/\Delta 3}$ fibroblasts formed colonies and grew on agarose culture. Notably, the IM1 fibroblasts formed colonies and the colonies became larger than colonies in IM3 fibroblasts. Both IM1 and IM3 fibroblasts had been cultured for more than 20 passages after transformed, while IM2 just transformed. From these results, it revealed that the transformed *Cspg2*$^{\Delta 3/\Delta 3}$ fibroblasts expressed anchorage-independent growth that is a character of malignant cell but non-transformed *Cspg2*$^{\Delta 3/\Delta 3}$ fibroblasts did not.

ลิขสิทธิ์มหาวิทยาลัยเชียงใหม่
Copyright© by Chiang Mai University
All rights reserved

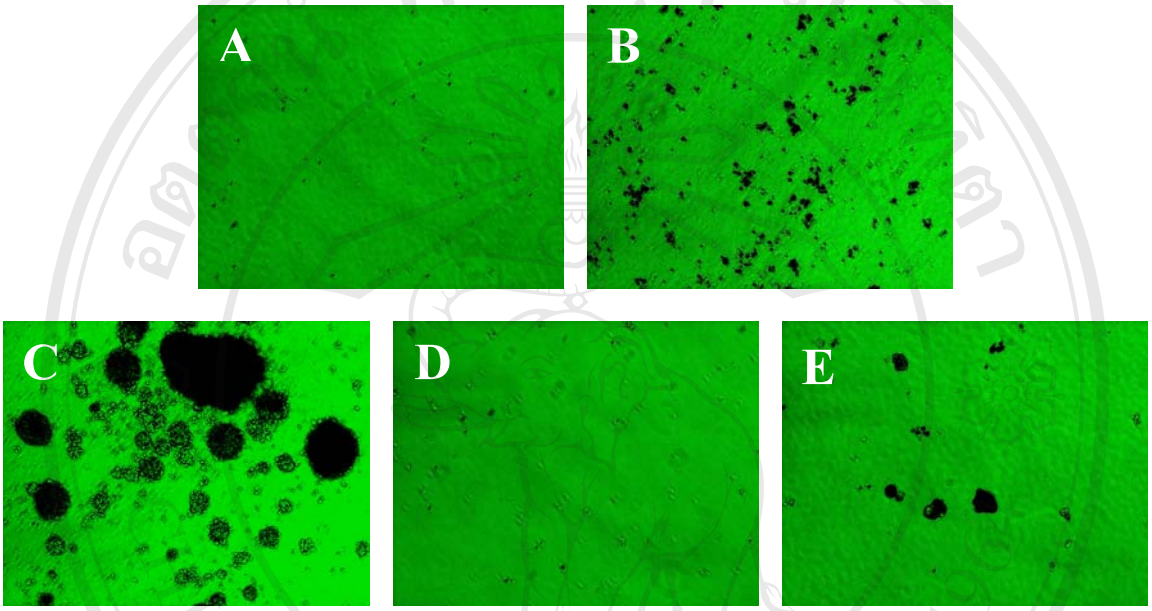

Figure 3.11 Colony formation assay. Fibroblasts were grown on 7% soft agarose gel culture. A = WT, B = early passages *Cspg2*$^{\Delta 3/\Delta 3}$, C = transformed *Cspg2*$^{\Delta 3/\Delta 3}$ (IM1), D = transformed *Cspg2*$^{\Delta 3/\Delta 3}$ (IM2), E = transformed *Cspg2*$^{\Delta 3/\Delta 3}$ (IM3).

ลิขสิทธิ์มหาวิทยาลัยเชียงใหม่
Copyright© by Chiang Mai University
All rights reserved

To confirm tumorigenicity ability of transformed *Cspg2*$^{\Delta 3/\Delta 3}$ fibroblasts, those fibroblasts were peritoneally injected into six weeks old BALB/c nu/nu slc mice (athymic or nude mice) to observe tumor formation, only malignant cells could generate tumor in these mice. The mice were grouped into two groups. Transformed *Cspg2*$^{\Delta 3/\Delta 3}$ fibroblasts (IM1, IM2, and IM3), and WT fibroblasts were injected into nude mice individually, they were noted as a first group. For second group, two lots of fibroblasts were transplanted into one mouse but at the different site. The results were illustrated in figure 3.12. For the first group, the IM1 fibroblasts as well as IM3 fibroblastsgenerated tumor node after for two weeks of implantation, but not IM3 which generated tumor around 5-7 weeks after implantation. However, tumor was not observed in IM2 fibroblasts. For WT fibroblasts, they did not promote tumor node generation in nude mice as expected. The second group showed similar result to the first one, in which both IM1 and IM3 fibroblasts were able to generate tumor but others failed. The tumor appearance was observed, those tumors became larger with erosion, necrosis with inflammation occurring at the end before mice were sacrificed to isolate their organs and tumor to further examine histological character.

ลิขสิทธิ์มหาวิทยาลัยเชียงใหม่
Copyright© by Chiang Mai University
All rights reserved

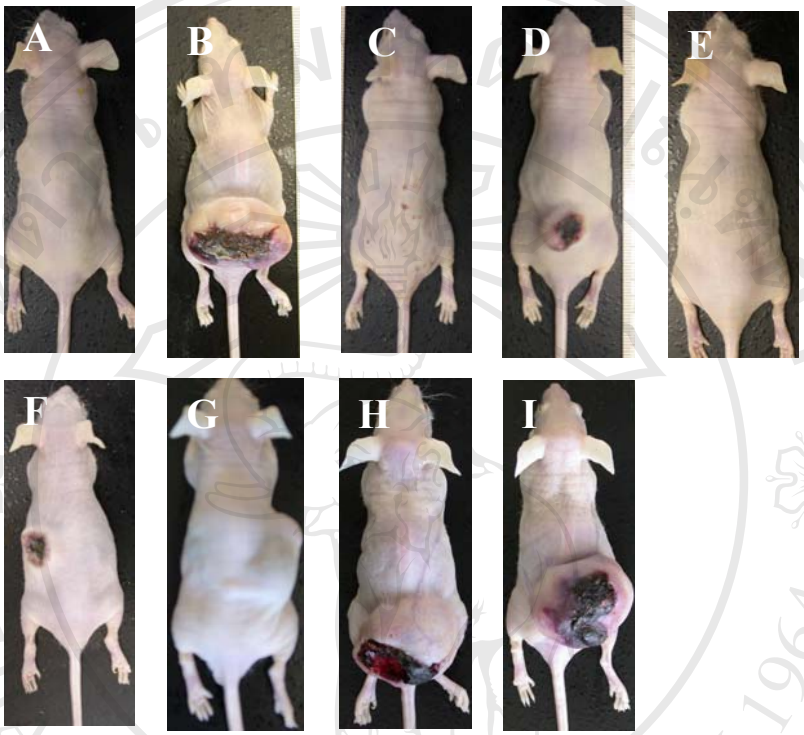

Figure 3.12 The tumor formation in BALB/c nu/nu mice. The transformed *Cspg2*$^{\Delta 3/\Delta 3}$ fibroblasts 1×10^{7} cells/ml were injected into the mice. A = WT, B = IM1, C = IM2, D = IM3, E = WT/IM2, F = WT/IM3, G = WT/IM1, H = IM3/IM1, I = IM2/IM1.

ลิขสิทธิ์มหาวิทยาลัยเชียงใหม่
Copyright© by Chiang Mai University
All rights reserved

Tumors from those mice were stained with hematoxylin and eosin to identify tumor characteristic. As shown in figure 3.13, the tumor consisted of a large number of fibroblastic cells with invasion into surrounding dermal tissue. At a higher magnification, the tumor cells were short and spindle-like, exhibiting a high nuclear/cytoplasmic ratio. These results clearly indicated that the transformed *Cspg2*$^{\Delta 3/\Delta 3}$ fibroblasts had characteristics of fibrosarcoma.

Beside, spleen size in tumor-bearing nude mice appeared a bit larger than normal. Metastasis from tumor to spleen and other organs was suspected, thus spleen and bone marrow from those mice were isolated and examined the abnormality. As shown in figure 3.13, there were no fibrosarcoma cells had been detected in spleen or bone marrow from tumor-bearing nude mice, it was assumed that there was no metastasis from tumor to other organs. Remarkably, there was no angiogenesis in those tumors, therefore necrosis of the tumor might come from lacking of nutrients to tumor.

ลิขสิทธิ์มหาวิทยาลัยเชียงใหม่
Copyright© by Chiang Mai University
All rights reserved

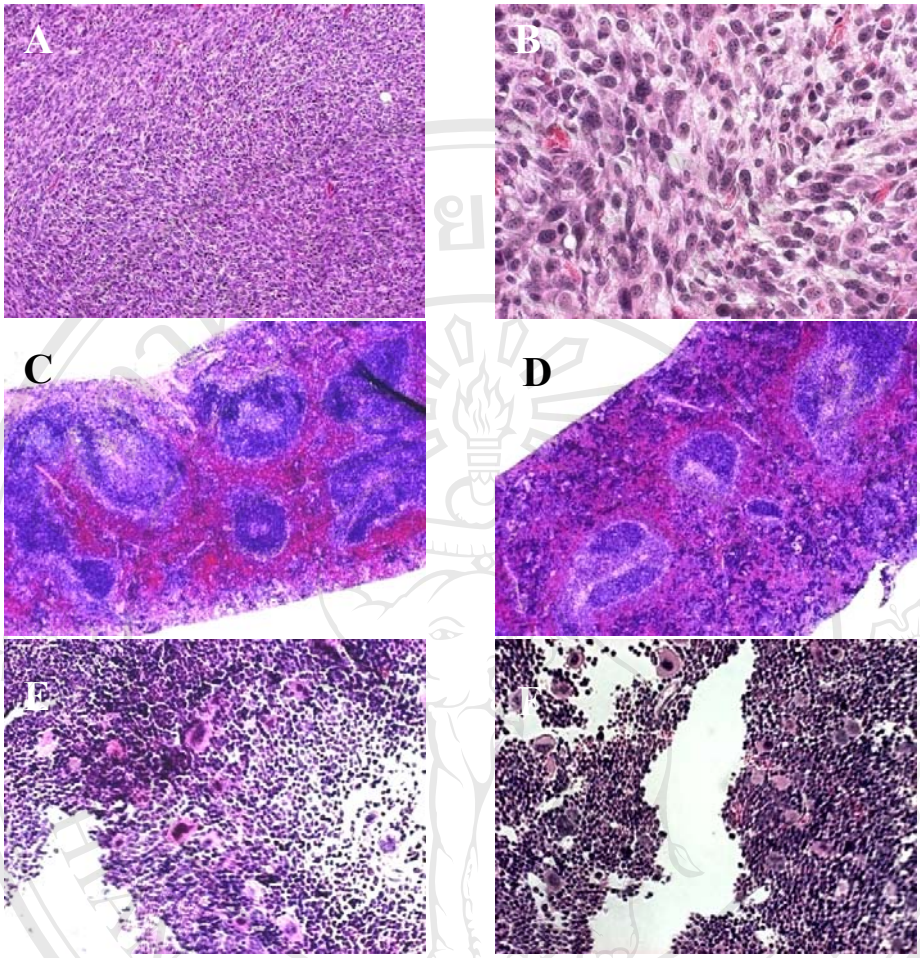

Figure 3.13 Hematoxylin & Eosin histological staining of tumors isolated from mice which injected with the *Cspg2*$^{\Delta 3/\Delta 3}$ fibroblasts, and spleen and bone marrow isolated from both mice which injected with the *Cspg2*$^{\Delta 3/\Delta 3}$ fibroblasts or WT fibroblasts at different magnification. A = tumor at 10X magnification, B = tumor at 40X magnification, C = spleen from WT fibroblasts injected mouse at 4X, D = spleen from the *Cspg2*$^{\Delta 3/\Delta 3}$ fibroblasts injected mouse at 4X, E = bone marrow from WT fibroblasts injected mouse at 20X, D = bone marrow from the *Cspg2*$^{\Delta 3/\Delta 3}$ fibroblasts injected mouse at 20X.

ลิขสิทธิ์มหาวิทยาลัยเชียงใหม่
Copyright© by Chiang Mai University
All rights reserved

3.1.5 Adhesion ability of the transformed *Cspg2*$^{\Delta 3/\Delta 3}$ fibroblasts.

Since versican plays a crucial role in an adhesion ability of cells to substratum, several studies have shown versican to interact with fibronectin, as well as collagen type I (Yamagata, Yamada et al. 1986) and that these interactions are responsible for reduced cell adhesion in melanoma cells (Touab, Villena et al. 2002). Fibronectin and collagen are integrin ligands and plays roles in enhancing cell adhesion. Similar to HA, major molecule that bind to versican and several proteins, helping to create a lattice that may regulate cell adhesion and migration (Toole 1990; Laurent and Fraser 1992). The defect in versican molecule might affect to adhesion ability of these mutant cells. To prove this suspicion, adhesion assay and cell attaching assay was performed. Adhesion assay was performed as described in 2.2.2.10, the early passages *Cspg2*$^{\Delta 3/\Delta 3}$ fibroblasts were not taken to perform this experiment because they grew slowly and have not enough cell number to perform a test. The result was shown in figure 3.14, all transformed *Cspg2*$^{\Delta 3/\Delta 3}$ fibroblasts adhered to uncoated plate better than WT fibroblasts, as well as fibronectin, laminin or type I collagen coated plate, however adhering ability to laminin coated plate was not different between IM1 and WT fibroblasts. This result revealed that defect in versican molecule might relate to adhesion ability of cell.

ลิขสิทธิ์มหาวิทยาลัยเชียงใหม่
Copyright© by Chiang Mai University
All rights reserved

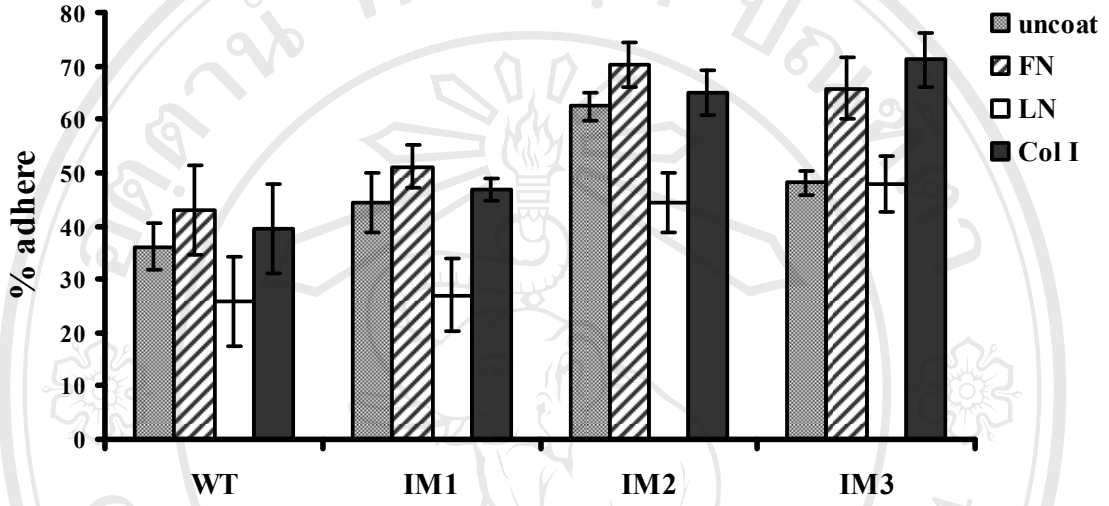

Figure 3.14 Adhering ability of the *Cspg2*$^{\Delta 3/\Delta 3}$ fibroblasts to various extracellular matrix molecules. Plates were coated with the extracellular matrix molecules including fibronectin, laminin, type I collagen and uncoated, then fibroblasts were plated to those coated or uncoated plates and adhering ability was determined. All values represent the mean $\pm$ SD in triplicate.

ลิขสิทธิ์มหาวิทยาลัยเชียงใหม่
Copyright© by Chiang Mai University
All rights reserved

3.1.6 Attaching ability of the *Cspg2*$^{\Delta 3/\Delta 3}$ fibroblasts

Other than adhering ability, attaching ability after the fibroblasts had been detached from substratum was determined. The transformed *Cspg2*$^{\Delta 3/\Delta 3}$ fibroblasts and the WT were detached from culture plate, then they were plated to culture plate again to observe attaching ability. The result showed in figure 3.15, all three lot of the transformed *Cspg2*$^{\Delta 3/\Delta 3}$ fibroblasts (IM1, IM2 and IM3) as well as the WT fibroblasts started attaching to culture plate at 2 hr after plated. However, the transformed *Cspg2*$^{\Delta 3/\Delta 3}$ fibroblasts began spreading at 4 hr and the spreading was completely done at 7 hr. There was no sign that the WT began spread at 4 or 7 hr. It was suggested that the transformed *Cspg2*$^{\Delta 3/\Delta 3}$ fibroblasts attached and spread on culture plate faster than the WT fibroblasts.

ลิขสิทธิ์มหาวิทยาลัยเชียงใหม่
Copyright© by Chiang Mai University
All rights reserved

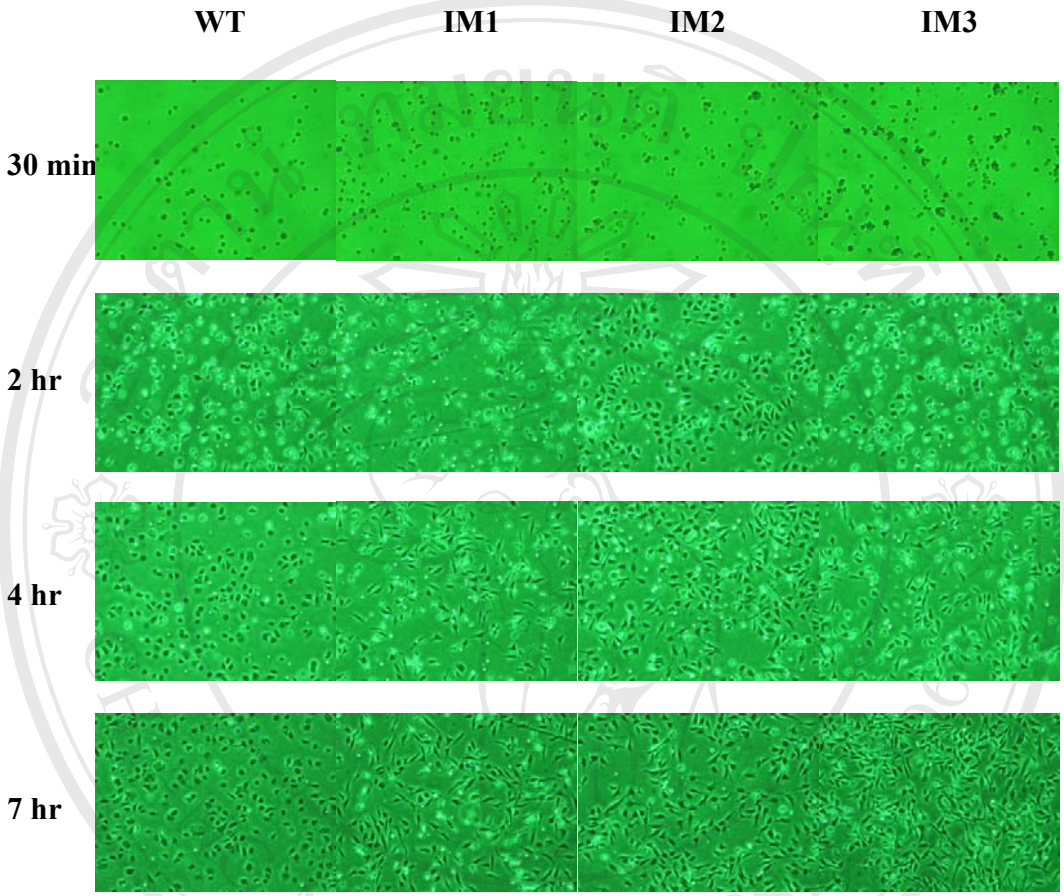

Figure 3.15 Attaching ability of fibroblasts to culture plate. Fibroblasts were plated on 35 mm culture dish containing DMEM with 10% FBS, 1% penicillin/streptomycin, then cells were photographed at 0.5, 2, 4, and 7 hr to observe attaching and spreading abilities.

ลิขสิทธิ์มหาวิทยาลัยเชียงใหม่
Copyright© by Chiang Mai University
All rights reserved

3.1.7 Exogenous versican adding to the *Cspg2*$^{\Delta 3/\Delta 3}$ fibroblasts did not recover cell proliferation rate to WT fibroblasts level.

According to proliferation rate and morphology of the A subdomain less versican (*Cspg2*$^{\Delta 3/\Delta 3}$) fibroblasts was different from the WT, it was expected that exogenous versican adding might recover proliferation rate or cell morphology of the *Cspg2*$^{\Delta 3/\Delta 3}$ fibroblasts to be the same as WT fibroblasts. To attest this postulate, versican was extracted from mice brain as described in 2.2.1.1. The extracted from mice brains composes of versican and aggrecan as a major proteoglycans. To separate aggrecan from versican, the extracted was added with CsCl, aliquoted into four tubes and then subjected to ultracentrifuge, after that the solution was fractionated into eleven fractions, fraction one was a bottom fraction and fraction eleven was a top fraction. Solutions from all eleven fractions were applied on nitrocellulose membrane and dot blot was performed to monitor aggrecan and versican in each fraction. Dot blot result was shown in figure 3.16, the upper figure represented a band positive to vesican and the lower figure represented a band positive to aggrecan. Versican positive bands dominantly presented in fractions 7-9, whereas aggrecan positive bands presented in fractions 2-5. The versican presenting fractions, fractions 7-9, were pooled and kept at -80˚ C for further use.

ลิขสิทธิ์มหาวิทยาลัยเชียงใหม่
Copyright© by Chiang Mai University
All rights reserved

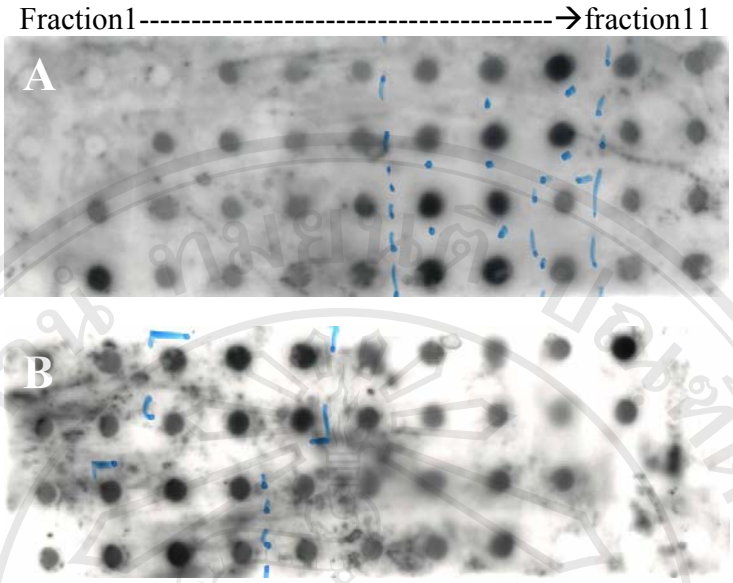

Figure 3.16 Dot blot analysis of versican and aggrecan which extracted from mice brain. CS-α chain and anti-aggrecan antibodies were used to detect versican (A) and aggrecan (B) respectively.

Fibroblasts were plated on 96 well culture plates at 1×10^4 cells/well, and the extracted versican was added to the culture to obtain the concentrations including 0, 2, 5, 20 µg/ml. The cultures had been cultured for two days before observed proliferation rate by BrdU ELISA proliferation assay. The result in figure 3.17 demonstrated that neither *Cspg2*$^{\Delta 3/\Delta 3}$ fibroblasts (mortal) nor transformed *Cspg2*$^{\Delta 3/\Delta 3}$ fibroblasts (IM1, IM2, IM3) proliferation rate were significantly changed after mice brain extracted versican had been added to the culture. Markedly, versican adding did not affect to the WT fibroblasts. Therefore, it was suggested that versican adding did not recover proliferation rate of fibroblasts which lacking A subdomain in versican molecule. It might be suggested that

ลิขสิทธิ์มหาวิทยาลัยเชียงใหม่
Copyright© by Chiang Mai University
All rights reserved

disruption of other versican related extracellular matrix molecules lead *Cspg2*$^{\Delta 3/\Delta 3}$ fibroblasts to change their behavior and morphology.

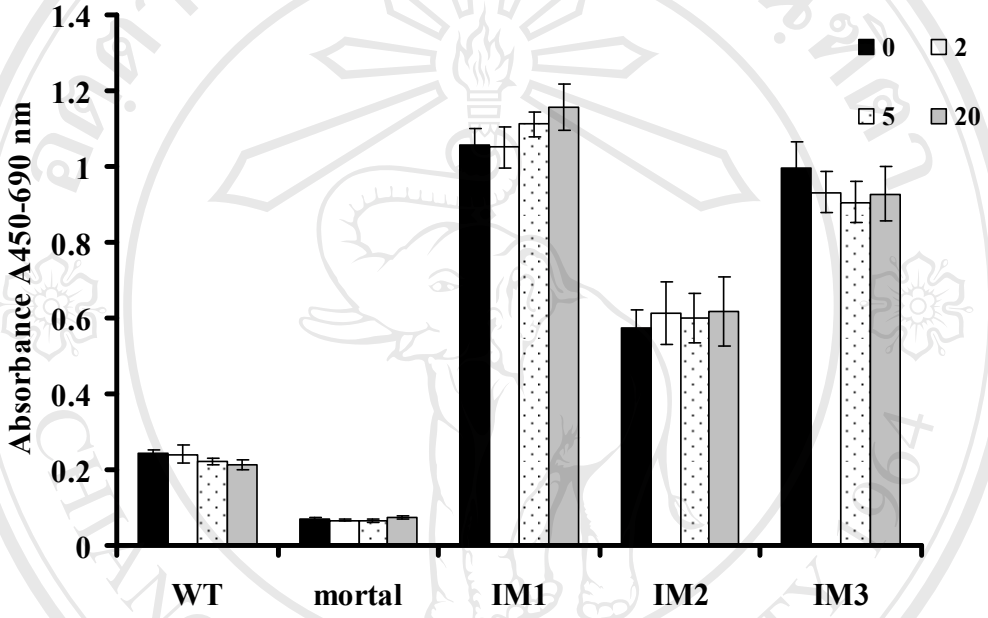

Figure 3.17 Proliferation rate of WT, *Cspg2*$^{\Delta 3/\Delta 3}$, and transformed *Cspg2*$^{\Delta 3/\Delta 3}$ fibroblasts which cultured in media containing different concentrations of mice brain extracted versican. Versican was added to DMEM media to obtain 2, 5, and 20 μg/ml final concentrations of versican, then the media were used to culture fibroblasts for two days, and observed proliferation rate. All values represent the mean ± SD in triplicate.

ลิขสิทธิ์มหาวิทยาลัยเชียงใหม่
Copyright© by Chiang Mai University
All rights reserved

3.2 Extracellular matrix proteins expression

Versican not only binds to HA, but also interacts to with several extracellular matrix molecules or receptors such as fibronectin, integrin, fibulin, fibrillin, tenascin, CD44, and EGF receptor (Wu, La Pierre et al. 2005). Altered expression or impaired structure of versican might affect to whole structure of extracellular matrix, and lead to cell morphology or behavior changing. In this studies, the A subdomain of versican molecule, known as enhancing interaction of versican and HA, was deleted. From observation, it apparently changed in cell behavior and morphology of the A subdomain less versican producing fibroblasts. It was hypothesized that the A subdomain deleting may break an interactions of versican and other extracellular matrix molecules, afterwards matrix structure, cell behavior and morphology was altered. To prove this hypothesis, expression as well as localization of versican and other extracellular matrix molecules in extracellular matrix was determined.

3.2.1 Versican expression decreased in the *Cspg2*$^{\Delta 3/\Delta 3}$ fibroblasts.

Versican expression had been observed in *Cspg2*$^{\Delta 3/\Delta 3}$ fibroblasts culture comparing with the WT fibroblasts. The fibroblasts were cultured, polyA RNA was collected, then reverse transcribed to cDNA, and subsequently real time RT-PCR was performed. The expression level of mRNA from both non-transformed and transformed *Cspg2*$^{\Delta 3/\Delta 3}$ fibroblasts showed only 25% and approximately 10 % of the WT fibroblasts expression level respectively as illustrated in figure 3.18. This result showed that lacking of the A subdomain from *Cspg2* gene caused dramatically decreasing of versican mRNA expression level. Interestingly, the expression continuously decreased in the transformed

ลิขสิทธิ์มหาวิทยาลัยเชียงใหม่
Copyright© by Chiang Mai University
All rights reserved

Cspg2$^{\Delta 3/\Delta 3}$ fibroblasts. However, localization of versican in extracellular matrix needed to be determined.

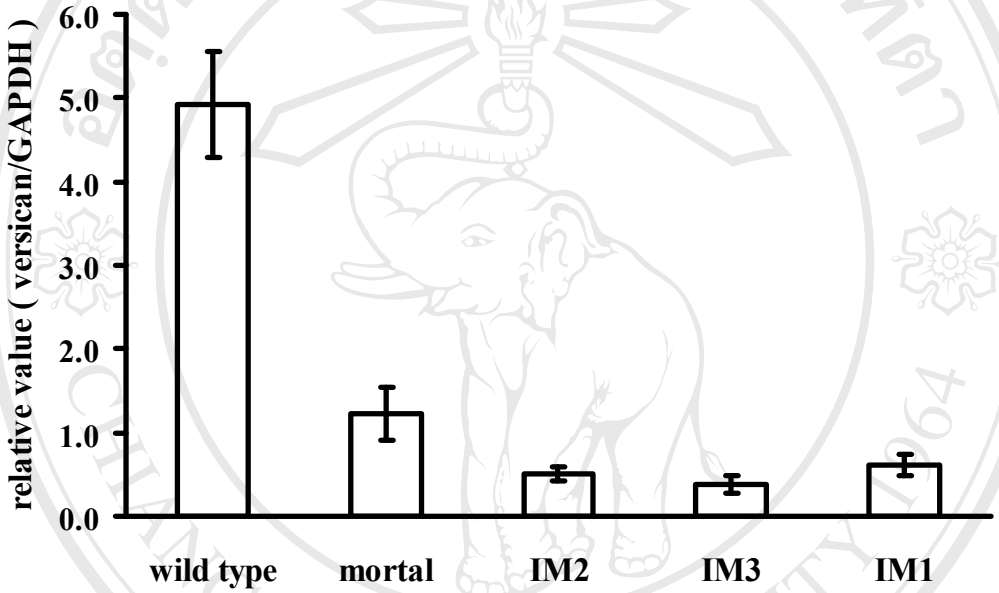

Figure 3.18 Expression level of versican mRNA in wild type, *Cspg2*$^{\Delta 3/\Delta 3}$ (mortal) and transformed *Cspg2*$^{\Delta 3/\Delta 3}$ (IM1, IM2, IM3) fibroblasts. Real time-RT PCR was performed to measure expression level of versican mRNA, GAPDH mRNA was used as an internal control. All values represent the mean $\pm$ SD in triplicate.

ลิขสิทธิ์มหาวิทยาลัยเชียงใหม่
Copyright© by Chiang Mai University
All rights reserved

3.2.2 Versican network in ECM was disrupted in the *Cspg2*$^{\Delta 3/\Delta 3}$ fibroblasts.

As demonstrated in 3.2.1, versican expression was decreased in the *Cspg2*$^{\Delta 3/\Delta 3}$ fibroblasts, to confirm result above, the localization of versican was determined. Fibroblasts were cultured in glass chamber slides until reached to confluence, and afterwards immunostaining to detect core protein of versican molecule was determined. As demonstrated in figure 3.19, the WT fibroblasts showed a dense bundle network of versican on the ECM, whereas the *Cspg2*$^{\Delta 3/\Delta 3}$ fibroblasts proliferated more slowly and did not reach the confluence, at ~90% confluence, they showed scattered immunostaining patterns with loss bundle network of versican. For the transformed *Cspg2*$^{\Delta 3/\Delta 3}$ fibroblasts, the IM1 was chosen to determine immunostaining pattern, at the confluence contained a larger number of cells and versican was only faintly immunostained with no appreciable network structure.

ลิขสิทธิ์มหาวิทยาลัยเชียงใหม่
Copyright© by Chiang Mai University
All rights reserved

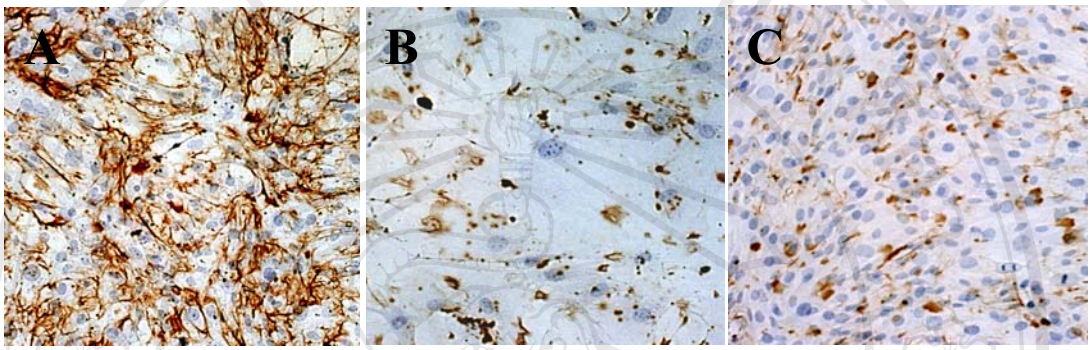

Figure 3.19 Localization of versican molecule in ECM of the WT (A), the *Cspg2*$^{\Delta 3/\Delta 3}$ (B), and the transformed *Cspg2*$^{\Delta 3/\Delta 3}$ (C) fibroblasts. Fibroblasts were cultured and stained with anti core protein of versican antibody. The immunostained cultures were photographed as 10X magnification.

ลิขสิทธิ์มหาวิทยาลัยเชียงใหม่
Copyright© by Chiang Mai University
All rights reserved

3.2.3 Chondroitin sulfate content in versican from the *Cspg2*$^{\Delta 3/\Delta 3}$ fibroblasts culture was decreased in the ECM but increased in cultured medium.

As the most proportion of chondroitin sulfate is derived from versican in proliferating fibroblasts (Hatano 2006), it was assumed that the level of chondroitin sulfate would reflect to the level of versican, thus chondroitin sulfate content and its pattern in cell layers and cultured media were determined. Fibroblasts were cultured until reached to confluence, and proteoglycan was extracted from cultured medium and cell layer. Proteoglycan was digested by chondroitinase ABC, afterwards chondroitin sulfate content and pattern was determined using HPLC.

Result showed that the WT fibroblasts presented a chondroitin 4-sulfate as a dominant isomer which found both in cell layer and cultured medium, while non-sulfate chondroitin sulfate was found as a minority. Remarkably, chondroitin 6-sulfate was found as a trace in cultured medium as shown in Table 2. It contrasted to chondroitin sulfate composition of versican which extracted from mice cartilage (Appendix D), as non-sulfated chondroitin sulfate and chondroitin 4-sulfate was found as majority and minority respectively. This result showed that versican from different organs contains different chondroitin sulfate isomers composition. Comparing between the WT and the *Cspg2*$^{\Delta 3/\Delta 3}$ fibroblasts cell layer, chondroitin 4-sulfated tended to decrease in the *Cspg2*$^{\Delta 3/\Delta 3}$ fibroblasts, but tended to increase in the transformed *Cspg2*$^{\Delta 3/\Delta 3}$ fibroblasts. In the cultured medium, not only chondroitin 4-sulfate and non-sulfate chondroitin sulfate, but chondroitin 6-sulfate were also found in versican extracted from the WT fibroblasts, the *Cspg2*$^{\Delta 3/\Delta 3}$ fibroblasts and the transformed *Cspg2*$^{\Delta 3/\Delta 3}$ fibroblasts. Remarkably,

ลิขสิทธิ์มหาวิทยาลัยเชียงใหม่
Copyright© by Chiang Mai University
All rights reserved

chondroitin sulfate E was found as a trace in the *Cspg2*$^{\Delta 3/\Delta 3}$ fibroblasts and transformed *Cspg2*$^{\Delta 3/\Delta 3}$ fibroblasts. The non-sulfate chondroitin sulfate in both *Cspg2*$^{\Delta 3/\Delta 3}$ and transformed *Cspg2*$^{\Delta 3/\Delta 3}$ fibroblasts had a tendency to decrease.

Considering to chondroitin sulfate content, chondroitin sulfate content of versican extracted from cell layer of the *Cspg2*$^{\Delta 3/\Delta 3}$ fibroblasts decreased three times comparing with the WT, data was illustrated in figure 3.20, and when the *Cspg2*$^{\Delta 3/\Delta 3}$ fibroblasts transformed, the chondroitin sulfate content dramatically decreased to 13 times of WT. In cultured medium, the *Cspg2*$^{\Delta 3/\Delta 3}$ fibroblasts cultured medium increased chondroitin sulfate content approximately 0.5 time, but when the *Cspg2*$^{\Delta 3/\Delta 3}$ fibroblasts transformed chondroitin sulfate content decreased to the same level as found in the WT fibroblasts cultured medium. Combining chondroitin sulfate content from cell layer and cultured medium together, it seemed no different between the WT and the *Cspg2*$^{\Delta 3/\Delta 3}$ fibroblasts chondroitin sulfate content, but when the *Cspg2*$^{\Delta 3/\Delta 3}$ fibroblasts transformed, the content decreased. From above results, it was suggested that when the A subdomain of versican was disrupted, versican molecules which anchoring to the ECM contained chondroitin sulfate content lesser than the proper versican (WT versican), whereas the *Cspg2*$^{\Delta 3/\Delta 3}$ versican which dissolved in the cultured medium contained chondroitin sulfate content more than the proper versican. However, when the *Cspg2*$^{\Delta 3/\Delta 3}$ fibroblasts transformed, chondroitin sulfate content in versican molecule was dramatically decreased. Remarkably, the disruption of the A subdomain might also alter chondroitin sulfate composition in versican molecule.

ลิขสิทธิ์มหาวิทยาลัยเชียงใหม่
Copyright© by Chiang Mai University
All rights reserved

Table 2. Chondroitin sulfate derived disaccharide composition in extracted proteoglycan from cell layers and cultured media of fibroblasts. The data was shown as % content.

	Cell layer			Medium		
	Wild type	Mortal	IM1	Wild type	Mortal	IM1
ΔdiOS	13	19	6	33	28	11
Δdi4S	87	81	94	59	59	80
Δdi6S	ND	ND	ND	8	12	9
ΔdiSE	ND	ND	ND	ND	1	1
ΔdiSD	ND	ND	ND	ND	ND	ND
ΔdiTriS	ND	ND	ND	ND	ND	ND

ลิขสิทธิ์มหาวิทยาลัยเชียงใหม่
Copyright© by Chiang Mai University
All rights reserved

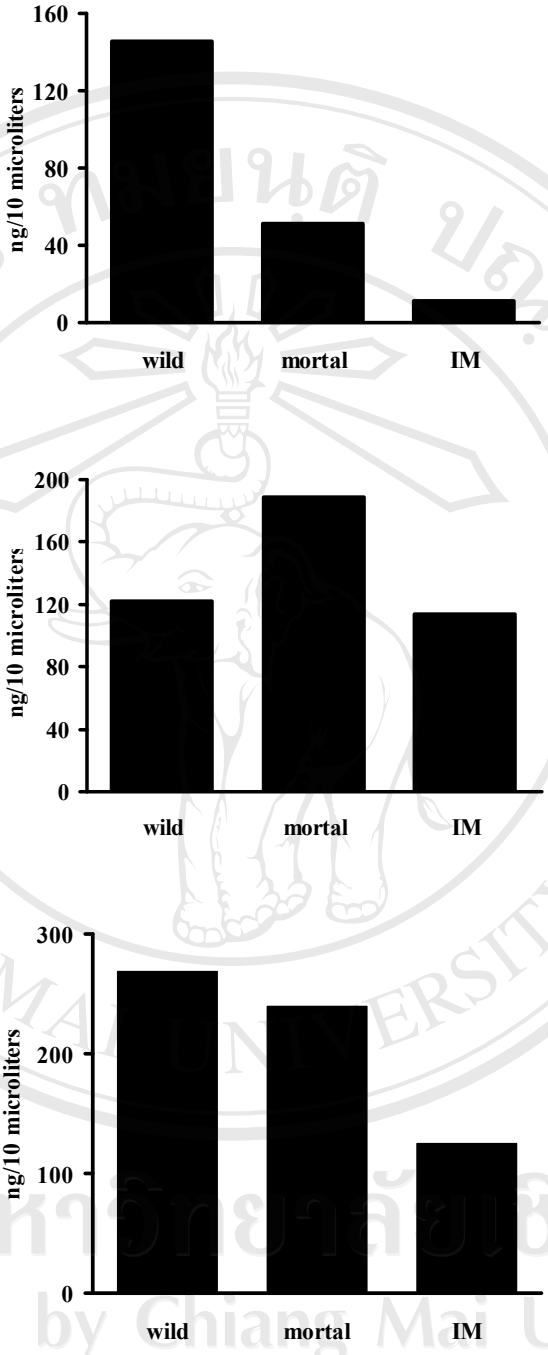

Figure 3.20 Chondroitin sulfate derived disaccharide content of extracted proteoglycan from cell layers (top) cultured media (center) and total content from cell layers and cultured media (bottom).

ลิขสิทธิ์มหาวิทยาลัยเชียงใหม่
Copyright© by Chiang Mai University
All rights reserved

3.2.4 HA deposition is altered in levels and structure in the Cspg2$^{\Delta 3/\Delta 3}$ fibroblasts.

Versican binds to HA at the B-B′ stretch of the G1 domain and the A subdomain of the G1 domain enhances the binding (Matsumoto, Shionyu et al. 2003), the absence of the A subdomain of versican in the *Cspg2*$^{\Delta 3/\Delta 3}$ presumably affects incorporation of HA in the ECM. Therefore, content and localization of HA in the *Cspg2*$^{\Delta 3/\Delta 3}$ fibroblasts cultures were determined. Fibroblasts cultures were stained with b-HABP, HA was observed as a network in the ECM in WT, whereas it was faintly stained on the cell surfaces in the *Cspg2*$^{\Delta 3/\Delta 3}$ fibroblasts culture, and rarely detected on the transformed *Cspg2*$^{\Delta 3/\Delta 3}$ cell culture as shown in figure 3.21. By HA-ELISA assay, as shown in figure 3.22 the contents of HA in the cell lysate including the ECM of the *Cspg2*$^{\Delta 3/\Delta 3}$ and the transformed *Cspg2*$^{\Delta 3/\Delta 3}$ cell culture were ~85% and ~20% of WT respectively, consistent with the staining intensity. The level of HA in the cultured medium was increased in the *Cspg2*$^{\Delta 3/\Delta 3}$ fibroblast culture, suggesting that HA is less incorporated and more accumulated in the condition medium. In contrast, level of HA had reduced in the condition medium of the transformed *Cspg2*$^{\Delta 3/\Delta 3}$ fibroblasts, indicating decreased HA synthesis. These results suggest an association of the decrease and altered HA-matrix assembly with the acquisition of the premature senescence and the autonomous growth in the *Cspg2*$^{\Delta 3/\Delta 3}$ fibroblasts.

ลิขสิทธิ์มหาวิทยาลัยเชียงใหม่
Copyright© by Chiang Mai University
All rights reserved

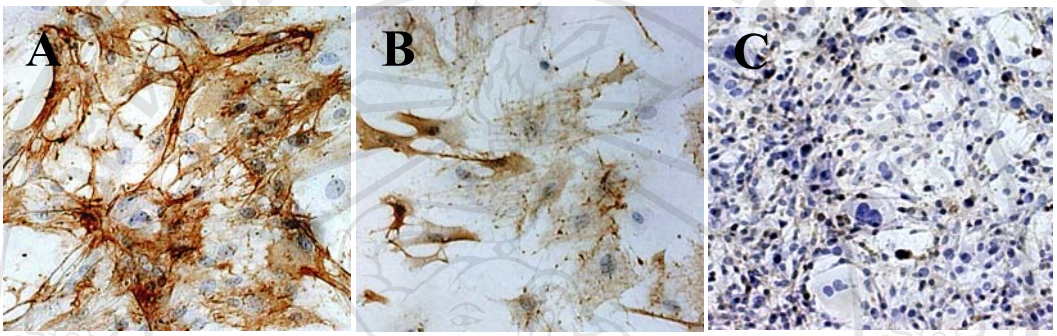

Figure 3.21 Localization of hyaluronan molecule in ECM of the WT (A), the *Cspg2*$^{\Delta 3/\Delta 3}$ (B), and the transformed *Cspg2*$^{\Delta 3/\Delta 3}$ (C) fibroblasts. Fibroblasts were cultured and stained with biotinylated hyaluronan binding protein (b-HABP). The immunostained cultures were photographed as 10X magnification.

ลิขสิทธิ์มหาวิทยาลัยเชียงใหม่
Copyright© by Chiang Mai University
All rights reserved

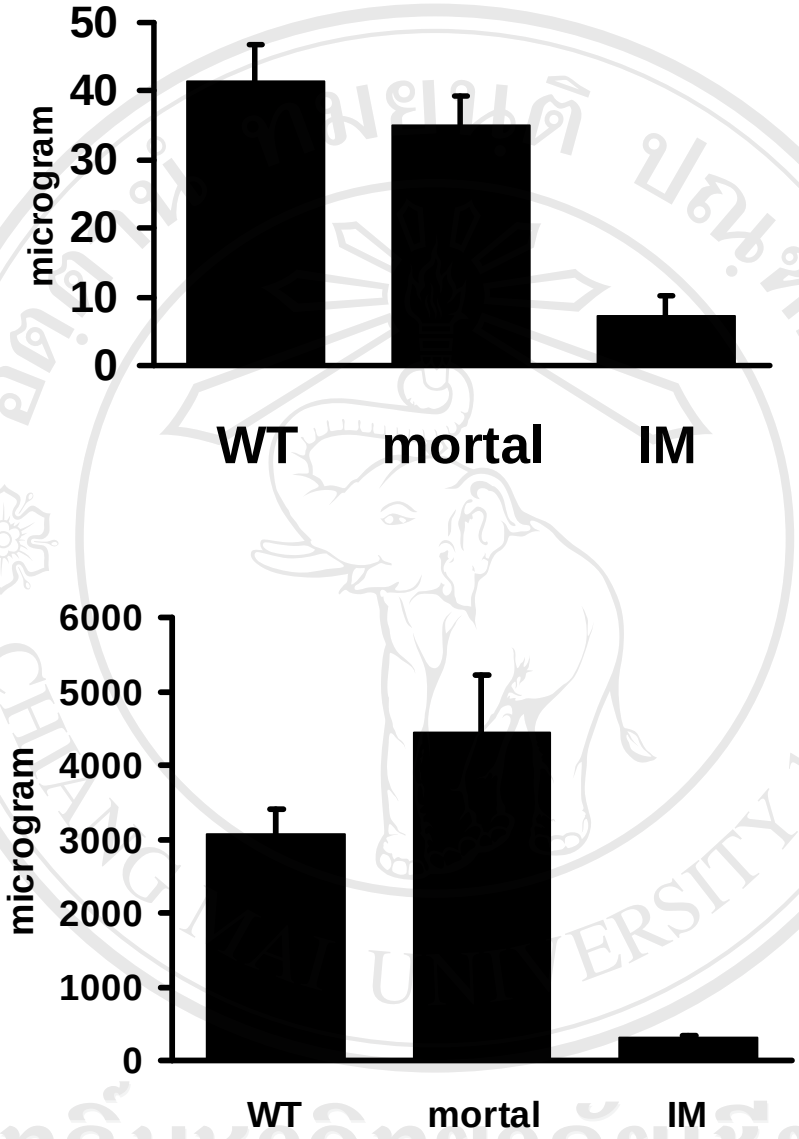

ลิขสิทธิ์มหาวิทยาลัยเชียงใหม่
Copyright© by Chiang Mai University
All rights reserved

Figure 3.22 Content of hyaluronan in cell layers (top), and cultured media (bottom) of fibroblasts cultures. Fibroblasts were cultured, then hyaluronan content was measured by HA-ELISA. All values represent the mean $\pm$ SD in triplicate.

3.2.5 Expression of fibronectin, laminin in the *Cspg2*$^{\Delta 3/\Delta 3}$ and the transformed *Cspg2*$^{\Delta 3/\Delta 3}$ cell cultures are comparable to the WT.

Fibronectin is known to regulate cell adhesion, and laminins are a major component of the basement membrane, which affect cell adhesion and tumor growth. Thus, their expression and localization in these fibroblast cultures need to be investigated. Western blot analysis and immunostaining was used to determine the expression level and localization respectively. The localization result was demonstrated in figure 3.23. For fibronectin, it showed a network structure in all the three cell types of fibroblast culture, although the structure appeared loose in the *Cspg2*$^{\Delta 3/\Delta 3}$ cell culture. While laminin was immunostained in a patchy pattern in WT, and in a dotted pattern of aggregates in the transformed *Cspg2*$^{\Delta 3/\Delta 3}$ fibroblast culture, whereas it was immunostained only faintly in the *Cspg2*$^{\Delta 3/\Delta 3}$ fibroblast culture. By western blot analysis as demonstrated in figure 3.24, the band density of both fibronectin and laminin was comparable among these three cell cultures, suggesting that the fainter immunostaining of both fibronectin and laminin in the *Cspg2*$^{\Delta 3/\Delta 3}$ cell culture might be due to a lower density of the cells. The immunostaining patterns and the expression levels of fibronectin and laminin were similar between WT and the transformed *Cspg2*$^{\Delta 3/\Delta 3}$ cells, these molecules are unlikely to affect the acquisition of autonomous growth in *Cspg2*$^{\Delta 3/\Delta 3}$ cells.

ลิขสิทธิ์มหาวิทยาลัยเชียงใหม่
Copyright© by Chiang Mai University
All rights reserved

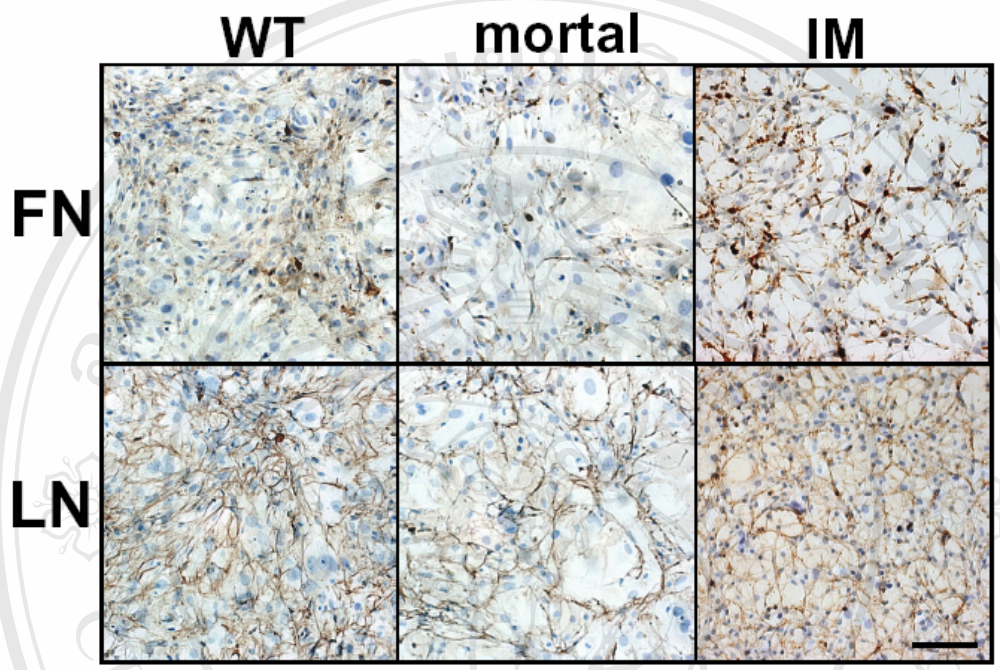

Figure 3.23 Localization of fibronectin (FN) and laminin (LN) in ECM of wild type (WT), the *Cspg2*$^{\Delta 3/\Delta 3}$ (mortal), and the transformed *Cspg2*$^{\Delta 3/\Delta 3}$ (IM) fibroblasts, fibroblasts were cultured and stained with anti-fibronectin and anti-laminin respectively. The immunostained cultures were photographed as 10X magnification.

ลิขสิทธิ์มหาวิทยาลัยเชียงใหม่
Copyright© by Chiang Mai University
All rights reserved

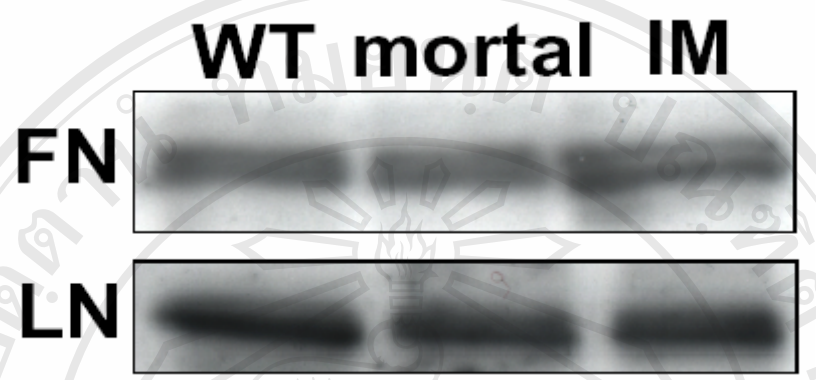

Figure 3.24 Expression of fibronectin (FN) and laminin (LN) from fibroblast cultures, the expression was determined by western blot analysis from cell lysates.

3.2.6 Collagen expression decreased in the *Cspg2*$^{\Delta 3/\Delta 3}$, but recovered in the transformed *Cspg2*$^{\Delta 3/\Delta 3}$ cells culture.

Type I collagen is a mainly molecule, which fibroblasts secret to ECM environment, it is important to be a scaffold structure for fibroblast cells. Thus, fibroblasts culture was immunostained for type I collagen in observing localization of this molecule. As shown in figure 3.25, staining in WT fibroblast culture, collagen formed network like structure, but in the *Cspg2*$^{\Delta 3/\Delta 3}$ and the transformed *Cspg2*$^{\Delta 3/\Delta 3}$ culture the network was looser than the WT. In detecting collagen expression, Sircol assay was used. The result in figure 3.26 showed that collagen expression was decreased, both in layer and conditioned medium of the *Cspg2*$^{\Delta 3/\Delta 3}$ culture, notably it was markedly reduced

ลิขสิทธิ์มหาวิทยาลัยเชียงใหม่
Copyright© by Chiang Mai University
All rights reserved

three folds from the WT in cell layer fraction. In the transformed *Cspg2*$^{\Delta 3/\Delta 3}$ fibroblasts, the collagen expression in cell lysate was recovered proximate to the WT expression level nevertheless, the expression still decreasing in conditioned medium and it was decreased lower than the non-transformed *Cspg2*$^{\Delta 3/\Delta 3}$ fibroblasts.

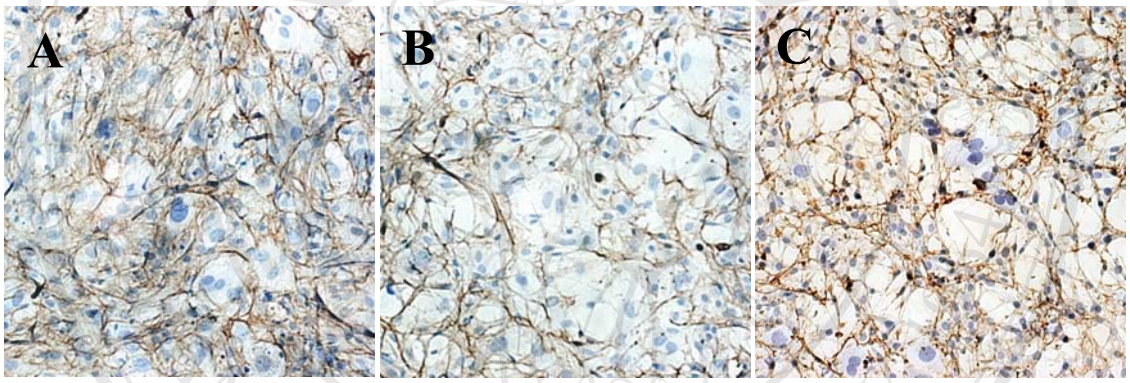

Figure 3.25 Localization of type I collagen in ECM of the WT (A), the *Cspg2*$^{\Delta 3/\Delta 3}$ (B), and the transformed *Cspg2*$^{\Delta 3/\Delta 3}$ (C) fibroblasts. Fibroblasts were cultured and stained with anti type I collagen antibody. The immunostained cultures were photographed as 10X magnification.

ลิขสิทธิ์มหาวิทยาลัยเชียงใหม่
Copyright© by Chiang Mai University
All rights reserved

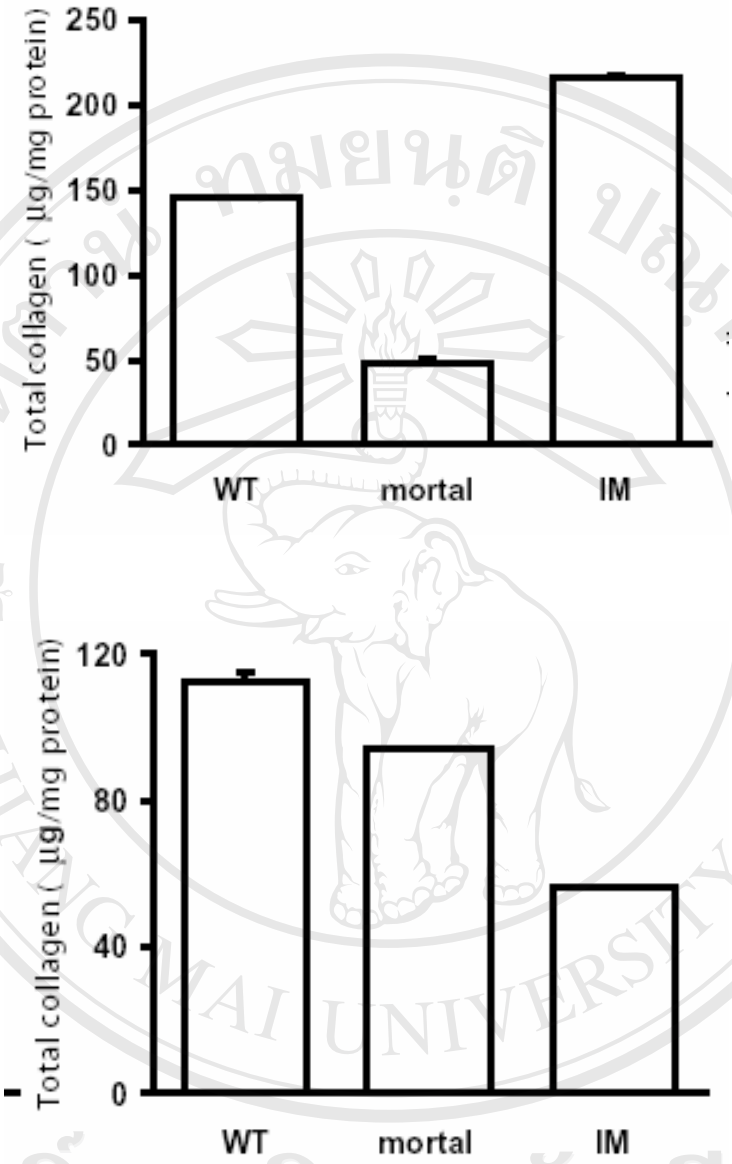

Figure 3.26 Content of collagen in cell layers (top), and cultured media (bottom) of fibroblasts cultures. Fibroblasts were cultured, then collagen content was measured by Sircol assay. All values represent the mean ± SD in triplicate.

ลิขสิทธิ์มหาวิทยาลัยเชียงใหม่
Copyright© by Chiang Mai University
All rights reserved

3.3 Signaling pathway elucidation

According to previous result, the *Cspg2*$^{\Delta 3/\Delta 3}$ fibroblasts at early passages grew very slowly and entered to senescent stage, and when growing them continuously they transformed to be tumor cells. To gain insight into the mechanisms underlying the slow proliferation and the subsequent anchorage-independent autonomous growth during the culture of the *Cspg2*$^{\Delta 3/\Delta 3}$ fibroblasts, expression of extracellular matrix related cell receptors and intracellular signaling proteins was elucidated.

3.3.1 p53 protein was upregulated in the *Cspg2*$^{\Delta 3/\Delta 3}$ fibroblasts, but abrogated in the transformed *Cspg2*$^{\Delta 3/\Delta 3}$ fibroblasts.

As expression of p53 serves as a marker of premature senescence and autonomous growth of cells, thus the expression of p53 had been investigated. By western blot analysis as shown in figure 3.27, the expression level of p53 in the *Cspg2*$^{\Delta 3/\Delta 3}$ fibroblasts was higher than that in WT fibroblasts. Interestingly, that in the transformed *Cspg2*$^{\Delta 3/\Delta 3}$ cells was rarely detected. This result corresponds to other reports that p53 was upregulated when cell entered to senescent stage, whereas it was downregulated when cell transformed to be a tumor.

ลิขสิทธิ์มหาวิทยาลัยเชียงใหม่
Copyright© by Chiang Mai University
All rights reserved

Figure 3.27 Expression of p53 protein in the WT (lane 1), the *Cspg2*$^{\Delta 3/\Delta 3}$ (lane 2), and the transformed *Cspg2*$^{\Delta 3/\Delta 3}$ (lane 3). Protein from cell lysate was subjected to SDS-PAGE, then western blot was performed, p53 was detected by enhanced chemiluminescent technique. Actin protein was used as internal control.

3.3.2 Phosphorylated ERK1/2 was upregulated in the *Cspg2*$^{\Delta 3/\Delta 3}$ fibroblasts, but downregulated in the transformed *Cspg2*$^{\Delta 3/\Delta 3}$ fibroblasts.

Lin A. W. (Lin, Barradas, et al. 1998) reported that premature senescence and transformation in fibroblasts involves p53 and constitutive MEK/MAPK mitogenic pathway. Therefore, MAPK pathway was suspected to be a downstream pathway responding to a signal from ECM of the *Cspg2*$^{\Delta 3/\Delta 3}$ fibroblasts culture. To attest this query, MAPK signaling molecules expression and phosphorylation had been observed. In figure 3.28, three major MAPK pathways proteins were determined by western blot analysis. It revealed substantial increase and decrease of phosphorylation levels of ERK1/2 in the *Cspg2*$^{\Delta 3/\Delta 3}$ fibroblasts and the transformed *Cspg2*$^{\Delta 3/\Delta 3}$ cells, respectively, compared with the WT fibroblasts. However, expression levels of total ERK1/2 were not

ลิขสิทธิ์มหาวิทยาลัยเชียงใหม่
Copyright© by Chiang Mai University
All rights reserved

altered in all three fibroblasts. For other MAPK pathway proteins, JNK/SAPK and p38, there were no alteration in both expression and phosphorylation levels of those proteins, compared with the WT fibroblasts. This result revealed that disruption of ECM structure in *Cspg2*$^{\Delta 3/\Delta 3}$ cell culture transmits a signal in to cell via ERK1/2 MAPK pathway.

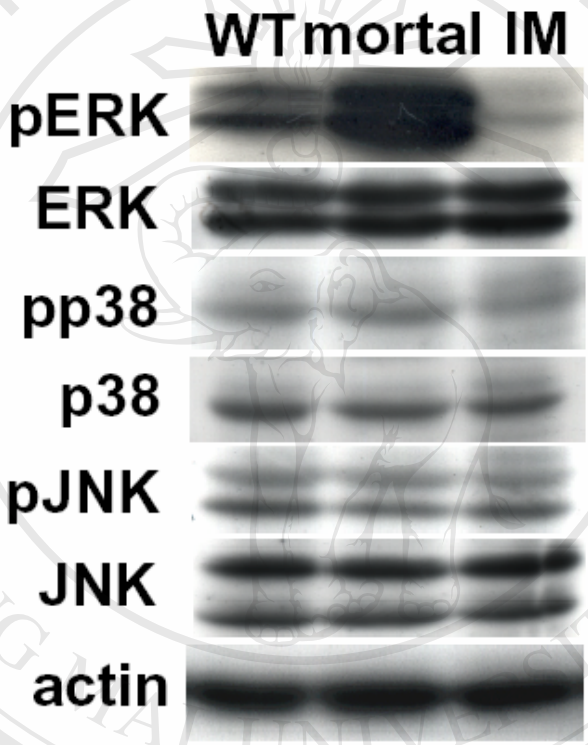

Figure 3.28 Expression of MAPK signaling protein in (ERK1/2, p38, JNK) the WT (lane 1), the *Cspg2*$^{\Delta 3/\Delta 3}$ (lane 2, mortal), and the transformed *Cspg2*$^{\Delta 3/\Delta 3}$ (lane 3, IM). Protein from cell lysate was subjected to SDS-PAGE, then western blot was performed, MAPK signaling protein was detected by ECL. Actin protein was used as an internal control.

ลิขสิทธิ์มหาวิทยาลัยเชียงใหม่
Copyright© by Chiang Mai University
All rights reserved

3.3.3 Phosphorylated ERK1/2 was regulated by the upstream molecules of the MAPK signal transduction cascade.

Since phosphorylation of ERK1/2 was upregulated and abrogated in the *Cspg2*$^{\Delta 3/\Delta 3}$ fibroblasts and the transformed *Cspg2*$^{\Delta 3/\Delta 3}$ fibroblasts, respectively. Hence, to investigate whether the phosphorylation of ERK1/2 actually is regulated by the upstream molecules of the signal transduction cascade, treatment of the upstream molecule inhibitor in MAPK pathway and a stimulus of MAPK pathway was performed. MEK1 inhibitor, PD98059 was used as MAPK pathway inhibitor. This substance inhibits MEK1, the upstream molecule of ERK1/2. After fibroblasts had been treated with PD98059, they were collected, and ERK1/2 expression was determined. The result in figure 2.29 demonstrated that the level of phosphoERK1/2 in WT fibroblasts substantially decreased. That in the *Cspg2*$^{\Delta 3/\Delta 3}$ fibroblasts, which had been higher than WT, slightly decreased. For the transformed *Cspg2*$^{\Delta 3/\Delta 3}$ fibroblasts, neither treated nor untreated cells appeared phosphorylated ERK1/2. The expression levels of total ERK1/2 were not altered in all three transformed fibroblasts. Next, EGF, a stimulus of MAPK pathway, was used to verify this signaling cascade. When treated with EGF, the level of phosphorylatedERK1/2 in WT fibroblasts substantially increased. That in the *Cspg2*$^{\Delta 3/\Delta 3}$ fibroblasts was no more elevated. In contrast, the phosphorylation of ERK1/2 was rarely observed in the transformed *Cspg2*$^{\Delta 3/\Delta 3}$ cells. These results suggest that the *Cspg2*$^{\Delta 3/\Delta 3}$ fibroblasts have the maximal level of ERK1/2 phosphorylation without EGF treatment, and that the transformed *Cspg2*$^{\Delta 3/\Delta 3}$ cells have escaped the regulation by the upstream molecules of the cascade.

ลิขสิทธิ์มหาวิทยาลัยเชียงใหม่
Copyright© by Chiang Mai University
All rights reserved

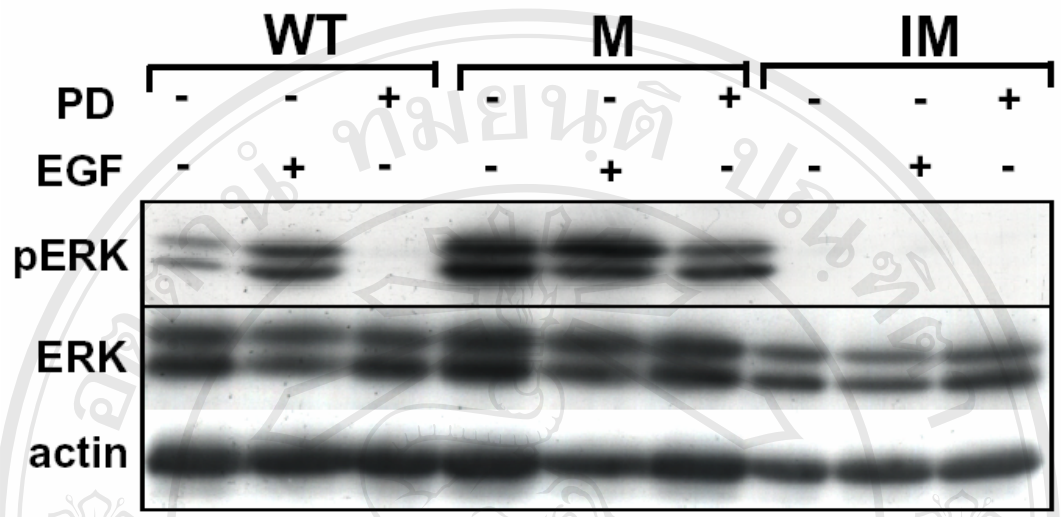

Figure 3.29 Effects of PD98059 and EGF to phosphorylation level of ERK1/2. Protein from cell lysate was subjected to SDS-PAGE, then western blot was performed, MAPK signaling protein was detected by ECL. Actin protein was used as an internal control.

3.3.4 Anti-CD44 suppressed ERK1/2 phosphorylation in the *Cspg2*$^{\Delta 3/\Delta 3}$ fibroblasts culture.

From previous observations implied that decreased the levels of versican deposition, and altered levels and assembly of HA in the ECM increased phosphorylation of ERK1/2, which may account for the altered behavior of the *Cspg2*$^{\Delta 3/\Delta 3}$ fibroblasts. Out of HA receptors on the cell surface, CD44 is known to mediate activation of ERK1/2 via Ras (Bourguignon, Gilad et al. 2006) (Cheng, Yaffe et al. 2006) (van der Voort, Taher et

ลิขสิทธิ์มหาวิทยาลัยเชียงใหม่
Copyright© by Chiang Mai University
All rights reserved

al. 1999). To investigate whether CD44 receptor involves phosphorylation of ERK1/2 in the *Cspg2*$^{\Delta 3/\Delta 3}$ fibroblasts, anti-CD44 monoclonal antibody was added to WT and the *Cspg2*$^{\Delta 3/\Delta 3}$ cell cultures. It was expected that CD44 receptor-HA binding on cell surface of the *Cspg2*$^{\Delta 3/\Delta 3}$ fibroblasts was blocked, then phosphorylation of ERK1/2 was decreased. When an anti-CD44 antibody was added to the WT culture medium for 2 hr, then activation of ERK1/2 was observed by immunostaining. The staining intensity of individual nuclei was unaltered in WT fibroblasts, whereas that was substantially diminished in the *Cspg2*$^{\Delta 3/\Delta 3}$ fibroblasts, as shown in figure 3.30. These results suggest that the decreased level and altered HA-matrix assembly in the ECM of *Cspg2*$^{\Delta 3/\Delta 3}$ fibroblasts culture transduced a signal to the cell via CD44 and elevated phosphorylation levels of ERK1/2.

ลิขสิทธิ์มหาวิทยาลัยเชียงใหม่
Copyright© by Chiang Mai University
All rights reserved

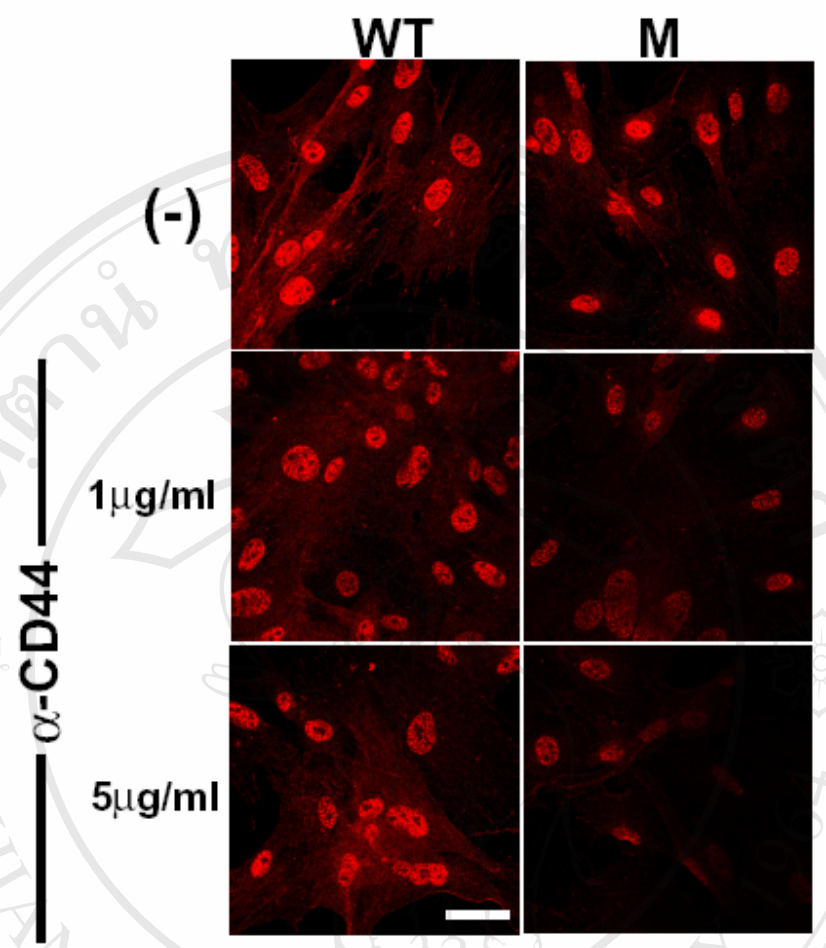

Figure 3.30 Effects of anti-CD44 treatment on phosphorylated ERK1/2. Both WT and the *Cspg2*$^{\Delta 3/\Delta 3}$ fibroblasts were cultured in the presence of an anti-CD44 antibody that block HA-CD44 interaction at 1 μg/ml or 5 μg/ml. Immunostaining patterns for phosphorylated ERK1/2 are shown (WT, wild type; M, the *Cspg2*$^{\Delta 3/\Delta 3}$ fibroblasts). Note that treatment with the antibody substantially diminishes the staining intensity for phosphorylated ERK1/2 in the senescent *Cspg2*$^{\Delta 3/\Delta 3}$ fibroblasts (Bar, 20 μm).

ลิขสิทธิ์มหาวิทยาลัยเชียงใหม่
Copyright© by Chiang Mai University
All rights reserved

3.3.5 HA-CD44 interaction mediated ERK1/2 phosphorylation in the hyaluronidase treated WT fibroblasts culture.

To substantiate that the HA-CD44 interaction mediates the ERK1/2 phosphorylation signal transduction, HA network in the ECM of WT fibroblasts was destroyed by hyaluronidase treatment. Then, the ECM structure of hyaluronidase treated WT fibroblasts mimics the ECM structure in the *Cspg2*$^{\Delta 3/\Delta 3}$ fibroblasts. As shown in figure 3.31, hyaluronidase at different concentrations was added to WT cell culture for 30 min and 2 hr, immunoblot analysis demonstrated significant increase of ERK1/2 phosphorylation by the hyaluronidase treatment. Furthermore, combined treatment with hyaluronidase and the anti-CD44 had been performed to confirm this assumption. The different concentrations of hyaluronidase were combined to 5 μg/ml anti-CD44, then added to the WT cell culture. Immunoblot analysis of phosphorylated ERK1/2 is demonstrated in Figure 3.32, it showed slight attenuation of ERK1/2 phosphorylation by the antibody. Taken together, these results suggest that the altered HA-matrix assembly by hyaluronidase treatment facilitates enhanced the CD44-mediated signal toward the phosphorylation of ERK1/2.

ลิขสิทธิ์มหาวิทยาลัยเชียงใหม่
Copyright© by Chiang Mai University
All rights reserved

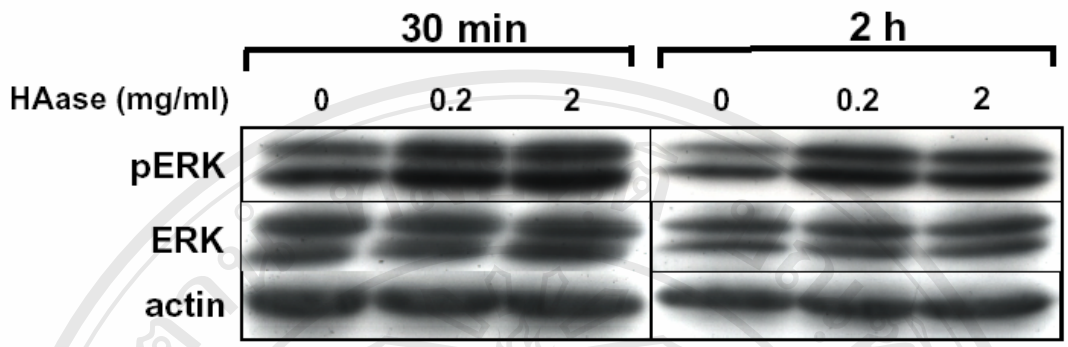

Figure 3.31 Effects of hyaluronidase treatment on phosphorylation of ERK1/2 in the WT fibroblasts. Cells were treated for the time periods at the concentrations as indicated and applied to immunoblot to detect phosphoERK1/2 (pERK), total ERK1/2 (ERK), and actin.

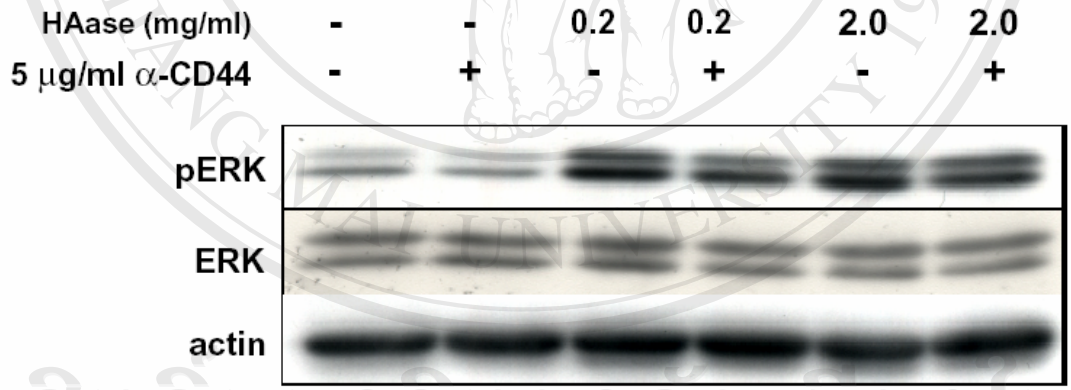

Figure 3.32 Effects of combined treatment with hyaluronidase and anti-CD44. The WT fibroblasts were treated with combinations of hyaluronidase and anti-CD44 for 30 min at the concentrations as indicated and applied to immunoblot to detect phosphoERK1/2 (pERK), total ERK1/2 (ERK), and actin.

ลิขสิทธิ์มหาวิทยาลัยเชียงใหม่
Copyright© by Chiang Mai University
All rights reserved

3.3.6 β1-integrin and EGF receptor did not involve ERK1/2 phosphorylation in the *Cspg2*$^{\Delta 3/\Delta 3}$ fibroblasts culture.

Versican has been shown to stimulate proliferation of NIH3T3 fibroblasts (Zhang, Cao et al. 1998). Recent studies have revealed that versican G3 domain interacts with β1-integrin and interfere with β1-integrin-EGF receptor interaction (Wu, Chen et al. 2004), the interaction between these two molecules transducer signal via ERK1/2. Therefore, to investigate whether β1-integrin and EGF receptor involves ERK1/2 phosphorylation in the *Cspg2*$^{\Delta 3/\Delta 3}$ fibroblasts, expression of β1-integrin and phosphorylated EGF receptor were determined. By western blot analysis, the expression level of β1-integrin was similar among WT, the *Cspg2*$^{\Delta 3/\Delta 3}$ fibroblasts, and the transformed *Cspg2*$^{\Delta 3/\Delta 3}$ cells. In addition, the phosphorylation level of the EGF receptor was also similar among these cell types, as shown in figure 3.33. Thus, it is unlikely that decreased versican directly attenuated cell proliferation by affecting the phosphorylation of ERK1/2.

ลิขสิทธิ์มหาวิทยาลัยเชียงใหม่
Copyright© by Chiang Mai University
All rights reserved

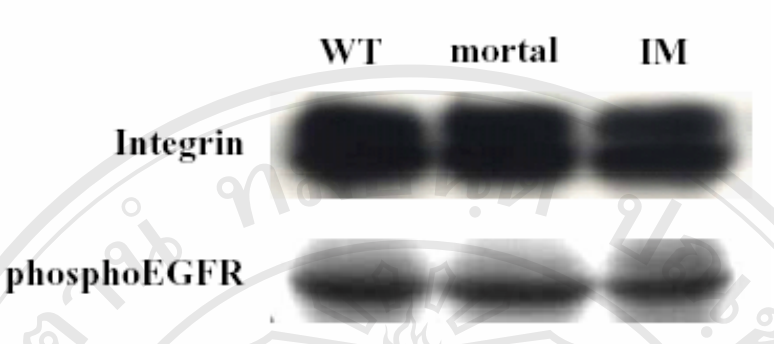

Figure 3.33 Expression of integrin (upper) and phosphorylatedEGFR (lower), the WT (lane 1), the *Cspg2*$^{\Delta 3/\Delta 3}$ (lane 2, mortal), and the transformed *Cspg2*$^{\Delta 3/\Delta 3}$ (lane 3, IM). Protein from cell lysate was subjected to SDS-PAGE, then western blot was performed, both integrin and phosphorylatedEGFR was detected by ECL.

3.3.7 Exogenous HA treatment enhanced the phosphorylation of ERK1/2.

Previous experiments strongly suggested that decreased versican reduces HA incorporation into the ECM and liberates free HA, which in turn facilitates its interaction with CD44 leading to phosphorylation of ERK1/2. To test this hypothesis, WT fibroblasts were treated with different sizes of HA (1000, 104, and 8 kDa) and different concentration (5, 50 and 150 μg/ml), then examined phosphorylation levels of ERK1/2. Immunoblot analysis as shown in figure 3.34 revealed that phosphorylation of ERK1/2 was elevated by the treatment with all the sizes of HA, but not depended to concentration. Thus, it is likely that interaction of free HA fragments with CD44 enhances ERK1/2 phosphorylation.

ลิขสิทธิ์มหาวิทยาลัยเชียงใหม่
Copyright© by Chiang Mai University
All rights reserved

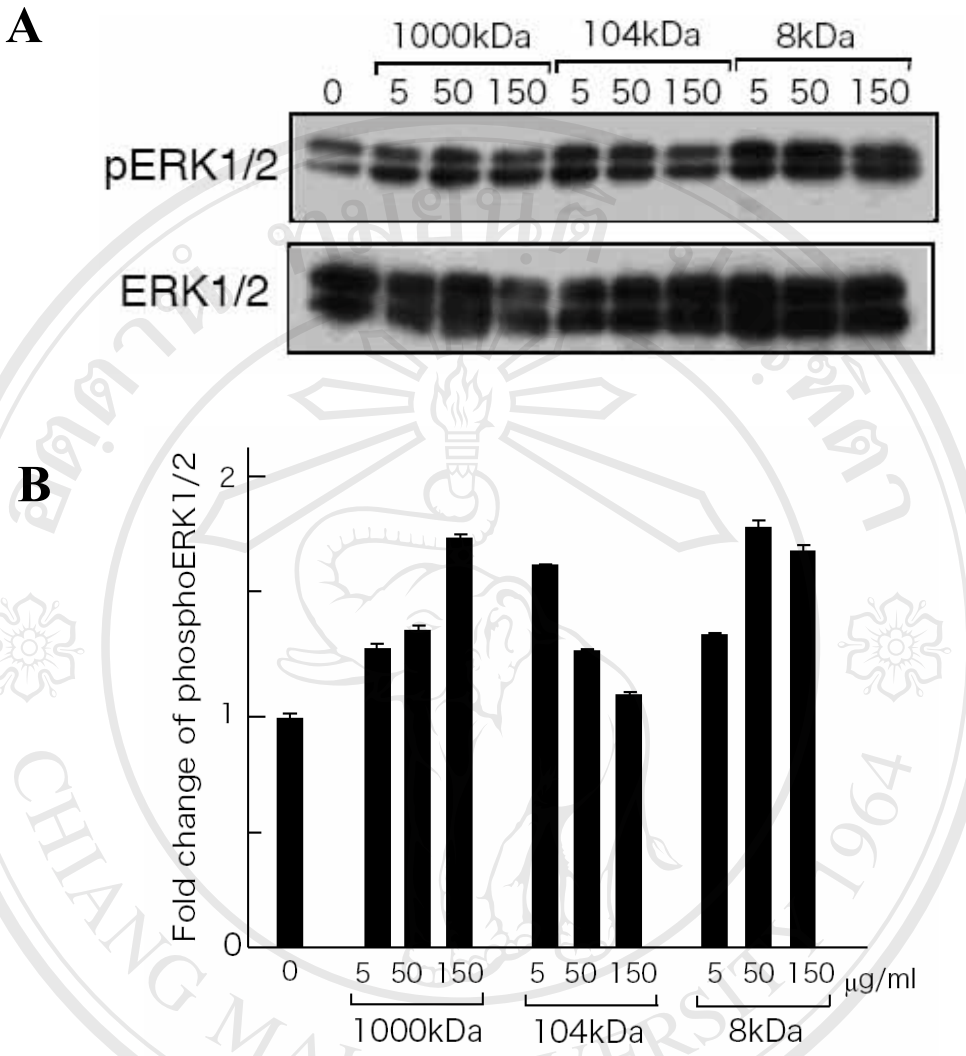

Figure 3.34 Effects of exogenous HA on phosphorylation of ERK1/2. WT fibroblasts were treated with different molecular sizes of HA at the concentrations as indicated for 16 h, and the cell lysates were applied to immunoblot. (A) Immunoblot patterns for phosphoERK1/2 and total ERK1/2 are shown. (B) The band density quantified by densitometry is indicated as fold changes of phosphoERK1/2. All values represent the mean ± SD from two experiments.

ลิขสิทธิ์มหาวิทยาลัยเชียงใหม่
Copyright© by Chiang Mai University
All rights reserved